

master's thesis

Mass Rate of Flow Virtual Sensor Inside the Air-Conditioning Unit

Artem Mishukov



May 2015

Supervisor: Ing. Vladimír Horyna

Czech Technical University in Prague
Faculty of Electrical Engineering, Department of Measurement



ZADÁNÍ DIPLOMOVÉ PRÁCE

Student: **Artem Mishukov**

Studijní program: **Inteligentní budovy**

Název tématu česky: **Virtuální senzor hmotnostního průtoku vzduchu uvnitř vzduchotechnické jednotky**

Název tématu anglicky: **Mass Rate of Flow Virtual Sensor Inside the Air-Conditioning Unit**

Pokyny pro vypracování:

Navrhněte a realizujte virtuální senzor hmotnostního průtoku vzduchu uvnitř vzduchotechnické jednotky obsahující rekuperační výměník. Virtuální senzor bude využívat pro odhad aktuální hodnoty hmotnostního průtoku běžně měřené teploty uvnitř komerčních vzduchotechnických jednotek, fyzikální vlastnosti rekuperačního výměníku a výkonovou charakteristiku rekuperačního výměníku. Pro vývoj, konfiguraci a testování virtuálního senzoru využijte experimentální vzduchotechnickou jednotku umístěnou v laboratoři katedry technických zařízení budov fakulty stavební ČVUT v Praze. V práci diskutujte možné přístupy k řešení dané problematiky, vyberte nejvhodnější metodu, kterou následně realizujete, a výsledky ověřte na reálné experimentální vzduchotechnické jednotce. Navrhněte a realizujte sérii měření, která umožní získat reálnou výkonovou charakteristiku rekuperačního výměníku obsaženého v uvedené experimentální vzduchotechnické jednotce, a tuto charakteristiku následně využijte jako jeden ze vstupních parametrů virtuálního senzoru.


Seznam odborné literatury:

- [1] *ASHRAE Handbook*. SI edition. Atlanta: American Society of Heating, Refrigerating and Air-Conditioning Engineers, 2010, 1 sv. (různé stránkování). ISBN 978-1-933742-82-3.
- [2] Roubal, J., Hušek, P.: *Regulační technika v příkladech*. 1. vyd. Praha: BEN - technická literatura, 2011, xxii, 276, ii s. ISBN 978-80-7300-260-2.
- [3] Jin, G.-Y. Cai, W.-J. Wang, Y.-W., and Yao, Y.: *A simple dynamic model of cooling coil unit*, Energy Conversion and Management, vol. 47, no. 15–16, pp. 2659–2672, Z 2006.

Vedoucí diplomové práce: Ing. Vladimír Horyna (K 13138)

Datum zadání diplomové práce: 15. ledna 2015

Platnost zadání do¹: 31. srpna 2016


Doc. Ing. Jan Holub, Ph.D.
vedoucí katedry




Prof. Ing. Pavel Ripka, CSc.
děkan

V Praze dne 15. 1. 2015

¹ Platnost zadání je omezena na dobu tří následujících semestrů.

Acknowledgement

I would like to thank my supervisor, Ing. Vladimír Horyna for his professional approach, unstinting support and guidance during whole course of this work. I would also like to express my appreciation to UCEEB and personally Ing. Daniel Adamovský, Ph.D. for his great help, informative consultations and provided access to laboratory.

Declaration

I declare that I worked out the presented thesis independently and I quoted all used sources of information in accord with Methodical instructions about ethical principles for writing academic thesis.

Abstract

Diplomová práce je zaměřena na vývoj virtuálních senzorů hmotnostního průtoku vzduchu uvnitř vzduchotechnických jednotek. Základní jádro virtuálního senzoru je tvořeno matematicky-fyzikálním modelem rekuperačního výměníku. Pro odhad hmotnostního průtoku vzduchu model využívá principy termodynamiky, mechaniky tekutin a přenosu tepla a byl realizován v prostředí Matlab a Simulink. Virtuální senzor byl testován na reálném laboratorním zařízení v různých provozních stavech vzduchotechnické jednotky. V závěru je diskutováno využití virtuálního senzoru pro komerční účely.

Klíčová slova

TZB; Technické zařízení budov; ventilace; klimatizace; Virtuální senzor; průtok vzduchu; rekuperátor

Abstract

This master thesis is focused on development of Virtual Sensor for mass flow rate measurements inside Air Conditioning Unit. Energy exchange process in heat recovery ventilator was chosen as physical basis for Virtual Sensor. Mathematical model of sensor utilizes principles of thermodynamics, fluid mechanics, and heat transfer and was constructed using Matlab and Simulink software. Results of modeling are evaluated with laboratory tests, during which impact of different factors on sensor's accuracy was studied. Furthermore, several scenarios for commercial implementation of the Virtual Sensor were introduced.

Keywords

HVAC; Heating; Ventilation; and Air Conditioning; AHU; ACU; Air Handling Unit; Air Conditioning Unit; Virtual Sensor; Airflow; Mass Flow; Recuperator

Contents

1	Introduction	1
1.1	Outline	1
1.2	Objectives	2
2	A literature review of deployed and developing solutions on virtual sensing	3
2.1	Methodology, history of development and categorization of VS	3
2.2	Virtual Sensors for HVAC systems in commercial buildings	5
2.3	Existing solutions of virtual airflow sensor for AHU	6
2.4	Summary	8
3	Theoretical basis and Virtual Sensor design	9
3.1	General information	9
3.2	Performance curves approach	10
3.2.1	Construction of the model in Simulink [®] software	11
3.3	Recuperator geometry approach	11
3.3.1	Construction of the model in Simulink [®] software	15
4	Evaluation of Virtual Sensor with Laboratory tests	17
4.1	Test rig configuration and parameters	17
4.1.1	Installed sensors	17
4.1.2	Parameters of heat exchanger	19
4.1.3	Performance curve measurement	19
4.2	Data processing	20
4.3	Transient state correction	20
4.4	Laboratory tests results	22
4.4.1	Long-term experiments	22
4.4.2	Short-term experiment 1 - high temperature difference	24
4.4.3	Short-term experiment 2 - medium temperature difference	24
4.4.4	Short-term experiment 3 - low temperature difference	25
4.5	Usage of alternative thermometers positions	27
4.5.1	Supply air temperature in front of HRV	29
4.5.2	Supply air temperature behind HRV	29
4.5.3	Exhaust air temperature in front of HRV	30
4.5.4	Exhaust air temperature behind HRV	30
4.5.5	Combination of alternative sensors	31
4.5.6	Combination of alternative sensors with corrections	31
4.6	Bypass leakage simulation	32
5	Scenarios of commercial utilization	34
5.1	Passive FDD algorithm	34
5.2	Active FDD algorithm	35
5.3	Implementation of VS on Programmable Logic Controller Tecomat Foxtrot	37
6	Conclusion	39
6.1	Discovered weaknesses and features of approach	39
6.2	Proposed improvements	40
	Bibliography	42

Appendices

A Simulink Diagram - Geometry approach	44
B Program for PLC source code	45

Symbols

Here main symbols description is given. Symbols with specifying indexes are explained in text.

b	linear dimension (m)
c_p	specific heat of the fluid (J/(kg*K))
\dot{C}	heat capacity rate of the fluid (W/K)
D_h	hydraulic diameter(m)
h	heat transfer coefficient (W/(m ² K))
k	gain coefficient (-)
L, l	linear dimensions (m)
MAT	mixed air temperature (°C)
n	number of channels (-)
Nu	Nusselt number (-)
Pr	Prandtl number (-)
\dot{Q}	rate of heat flow (W)
Re	Reynolds number (-)
S	area (m ²)
SAT	supply air temperature (°C)
SHR	sensible heat ratio(-)
t_s	temperature of supply air in front of HRV
t'_s	temperature of supply air behind HRV
t_e	temperature of exhaust air in front of HRV
t'_e	temperature of exhaust air behind HRV
TTE	Temperature Transfer Efficiency
u	velocity of flow (m/s)
\dot{V}	volumetric air flow rate (m ³ /s)
α	thermal diffusivity of fluid (m ² /s)
δ	thickness (m)
ΔT	change in temperature (K)
ΔT_m	logarithmic mean temperature difference (LMTD)
η	fins efficiency (-)
λ	thermal conductivity (Wm ⁻¹ K ⁻¹)
ν	kinematic viscosity (m ² /s)
ρ	air density (kg/m ³)

List of Figures

1	The Classification of Virtual Sensors. [2]	3
2	Main phases of VS developing process [2].	4
3	Systemization of virtual sensors [2].	6
4	A scheme of deployment a virtual flow rate meter. [4]	7
5	Generic scheme of recuperator (winter mode).	9
6	Diagram of Virtual Sensor - Performance curves approach	12
7	Heat exchange process in recuperator.	13
8	Plate geometry	14
9	Simplified diagram of Virtual Sensor - Recuperator geometry approach	15
10	AHU testing rig	17
11	Block arrangement of AHU test rig. [16]	18
12	Performance curve of test rig	19
13	Input data filtration (Exhaust air)	20
14	Supply mass airflow temperature settling	21
15	Supply mass airflow transient states corrected	21
16	Temperature readings - experiment 20.02.2015-10.03.2015	22
17	Exhaust mass airflows - experiment 20.02.2015-10.03.2015	23
18	Supply mass airflows - experiment 20.02.2015-10.03.2015	23
19	Exhaust mass airflows - experiment 1.04.2015	25
20	Supply mass airflows - experiment 1.04.2015	25
21	Exhaust mass airflows - experiment 13.04.2015	26
22	Supply mass airflows - experiment 13.04.2015	26
23	Exhaust mass airflows - experiment 5.05.2015	27
24	Supply mass airflows - experiment 5.05.2015	27
25	Exhaust mass airflows - experiment 5.05.2015 - filtered	28
26	Supply mass airflows - experiment 5.05.2015 - filtered	28
27	Temperatures during 1.4.2015 experiment	29
28	1.4.2015 experiment - Thermometer 1	29
29	1.4.2015 experiment - Thermometer 6	30
30	1.4.2015 experiment - Thermometer 11	30
31	1.4.2015 experiment - Thermometer 10	31
32	1.4.2015 experiment - Thermometers 1, 11 and 10	31
33	1.4.2015 experiment - Thermometers 1, 11 and 10 with corrections	32
34	Exhaust mass airflows - open bypass	33
35	Supply mass airflows - open bypass	33
36	FDD algorithm scheme - passive method	35
37	FDD algorithm scheme - active method	36
38	Tecomat Foxtrot Central Unit CP-1000 [18]	37
39	Virtual sensor model in CFC language	38
40	Web interface of FDD system	38

41	Overall Simulink diagram - geometry approach.	44
----	---	----

1 Introduction

Though sufficiently big number of researches has been carried out to date on Fault detection and diagnostics (FDD), functionality of modern FDD systems for building technologies (eq. Heating, Ventilation and Air Conditioning or HVAC) is distinctly restricted by disposable sensors. Majority of solutions is based solely on temperature measurements, set-points and control signals. [1] Those limitations are dictated mostly by cost-efficiency and not specific for exact type of FDD method. Researchers suggest to solve that problem by using so-called Virtual Sensors. [2]

Virtual Sensors (VS), also known as soft sensors, are used to estimate quantity by means of lower cost physical sensors and mathematical models. It can be useful when measurement of quantity is expensive or physically difficult to provide. [3]

Virtual airflow sensor for Air Conditioning Unit (ACU) was chosen as subject of this study. Since physical flow sensors are rarely being installed in field applications due to lack of space in ACU, fragility, high cost and ineffectiveness, supply airflow usually remains unmeasured. [4] On the other hand, this is essential parameter for determination of energy balance in the system. [5] It could also be used to detect unnecessary cooling or heating or as additional input for advanced control system.

Remark: concept of Air Handling Unit (AHU) is also often used in literature, strictly speaking main difference between ACU and AHU is that first one has components for air humidity alteration and chiller whereas AHU does not necessary have those elements. Although often those concepts can be interchangeable.

Unique method of air flow rate estimation will be based on heat exchange process inside recuperator.

1.1 Outline

This work is divided into six thematic parts.

In Introduction work description and objectives are given.

In the second chapter brief methodology, history of development and categorization of Virtual Sensors is introduced, then state-of-the-art literal research in virtual sensing for building technologies is presented.

Chapter 3 describes physical principles on which Virtual Sensor is based, also model of sensor is designed using Simulink software.

In Chapter 4 sensor has been evaluated with laboratory tests, certain adjustments have been made to computational methods according to tests results.

In Chapter 5 examples of sensor utilization have been given, also models from chapter 3 were converted to program code for Programmable Logical Controller.

Chapter 6 concludes this thesis and proposes improvements of the Virtual Sensor for future research.

1.2 Objectives

This section briefly describes main objectives of the thesis:

- Determine current state-of-the-art in virtual sensing for building technologies and compare it to other fields.
- Present theoretical basis for supply airflow virtual sensor.
- Derive necessary physical dependencies inside recuperator from basic thermodynamic equations.
- Design mathematical model (virtual sensor) of recuperator based on that relations using Matlab and Simulink software.
- Evaluate model with laboratory tests in different conditions, simulating unit failures and air flow rate changes
- Propose scenarios for commercial implementation of the Virtual Sensor
- Extract method's weaknesses and propose ways to improve sensor in future research

2 A literature review of deployed and developing solutions on virtual sensing

This chapter introduces in brief methodology, history of development and categorization of Virtual Sensors. It also contains state-of-the-art in virtual sensing for building technologies.

2.1 Methodology, history of development and categorization of VS

Application of virtual sensing techniques in commercial buildings could facilitate the development of more cost-effective and robust diagnostic systems and optimal control what in turn can save up to 50% from energy penalties and reduce service costs by up to 70%. [6]

An overall review of available VS solutions for HVAC was written by Li, Yu and Braun. [2] Rapid development of virtual sensing technology started over decade ago, predominantly from researches in process controls and automobiles. In this fields VS are commonly used for estimation such quantities as vehicle velocity [7] or vehicle tire air pressure. [8]

Virtual sensors can be categorized according to three interrelated criteria: measurement characteristics, modeling methods, and application (Fig. 1). [2]

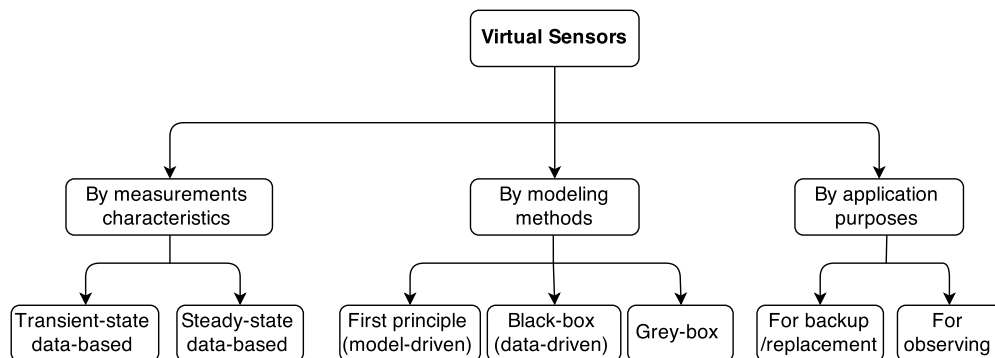


Figure 1 The Classification of Virtual Sensors. [2]

The measurement characteristic category refers to whether the desired virtual sensor outputs are transient or steady-state variables. A transient virtual sensor incorporates a transient model to predict the transient behavior of an unmeasured variable in response to measured transient inputs. With respect to modeling methods, virtual sensors can

be divided into three types: first-principle (model-driven), black-box (data-driven), and gray-box virtual sensors. In **data-driven** methods diagnostic rules are derived statistically from large amount of measured data. Data is processed in «black-box» style, so no deep physical understanding of system is required. On the other hand, such FDD systems can only diagnose faults presented in training data. Most commonly implemented and well-studied are **model-based** approaches. Those methods utilize mathematical models, usually constructed from first principles. **Gray-box** virtual sensors are also based on first principles (sometimes simplified) although also contain number of unknown free parameters which can be estimated using system identification. [2]

According to application, virtual sensors can be divided into backup/replacement and observing virtual sensors. **Backup/replacement** virtual sensors are used either to back up or replace existing physical sensors. In contrast, **observing virtual sensors** estimate quantities that are not directly measurable using existing physical sensors. [2]

To develop **transient-state** VS, responses to rapid control changes are measured. Physical, gray-box or black-box models can be used. Transient physical or gray-box models are usually represented by sets of linear or nonlinear differential equations or time-series equations. As apposed, **steady-state** VSs are developed using measurements collected while a system is running in an uninterrupted, continuous way. Steady-state virtual sensors use algebraic equations rather than differential or time-series equations and respond instantaneously to time-varying inputs to provide quasi-steady outputs. Steady-state virtual sensors can use physical, gray-box, or black-box models as well. Steady-state first principle models might incorporate mass balances, force balances, energy balances which describe a mechanical, thermal, or chemical processes. Black-box models are often multi-variable polynomials or neural networks.

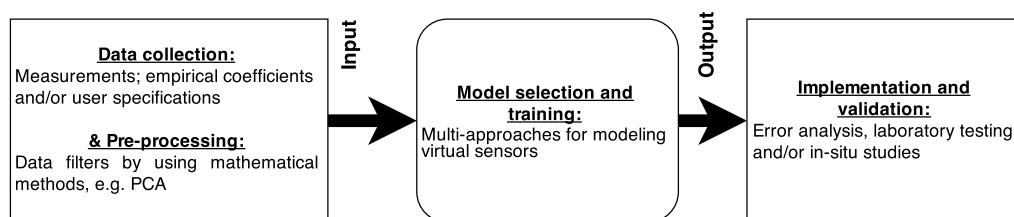


Figure 2 Main phases of VS developing process [2].

According to Li, Yu and Braun developing of VS is domain-specific process, generally, it can be divided into three phases: data collection and pre-processing, model selection and training, and sensor implementation and validation (Fig. 2). **Data collection and pre-processing** strongly affects accuracy and reliability of VS and should be provided according to chosen modeling approach. **Model selection and training** are the most difficult and critical steps in the process of developing virtual sensor. There are many model types to choose from, and each requires a process of determining the proper model order, estimating parameters, and then redefining the model selection/order. A virtual sensor could be **implemented** as part of a control or monitoring system or as a standalone sensor with its own hardware, embedded software, and input/output channels. In either case, the virtual sensor implementation needs to be tested in both laboratory and in-situ studies to validate performance and evaluate robustness.

2.2 Virtual Sensors for HVAC systems in commercial buildings

Virtual sensing technology for HVAC is still in its infancy, since active attempts to develop such tools started at second half of 2000s. Most of existing solutions functions as first principle or gray box models and employs steady state measurements (usually from low-cost temperature sensors together with manufacturer's rating data). Commonly such virtual sensors were used to estimate missing quantities for purposes of FDD systems, rather than to replace or back up available physical sensors. Examples of such virtual sensors will be presented in this chapter.

One of the first papers was written by Ward and Siegel and was concerned with virtual filter efficiency sensor. [9] The proposed idea was to apply the measured pressure drop of the filter to determine the airflow through the bypass cracks and accounts for particle loss in the bypass cracks. In order to quantify bypass flow, a quadratic relationship was employed to relate flow to pressure drop in a rectangular sharp-edged crack. The results shown significance of filter efficiency tracing, since accruing hardly visible gasps can dramatically affect performance of filters. As a conclusion laboratory tests was advised for verification of model.

Li and Baun presented series of papers dedicated to sensors for vapor compression air-conditioners with the main purpose of reducing costs for an FDD method. [10] Eleven virtual sensors were developed and validated during researches for major components of vapor compression system: compressor, condenser, and expansion valve. For instance, a virtual refrigerant charge sensor was introduced due to fact, that more than 50% of the air-conditioning systems in the field have improper refrigerant charge and also there is no direct measurement of refrigerant charge besides removing all of the charge and weighing it. This VS utilizes steady state measurements from four surface mounted temperature sensors. The algorithm for estimating refrigerant charge from temperature measurements uses simple algebraic equations derived from thermodynamic laws. This virtual refrigerant charge sensor algorithm has been validated for a range of different systems and over a wide range of operating conditions with and without other faults. Reported charge predictions were within 8% of the actual charge.

Virtual sensors were also developed for heat pumps. Li and Braun proposed and tested virtual check-valve leakage sensor. [11] This VS employed upstream and downstream pressure measurements on par with refrigerant mass flow which in turn was estimated by virtual refrigerant mass flow rate sensor. Some laboratory evaluations were performed to evaluate diagnostic performance using these leakage indicators, and it was found that faults could be identified before heating capacity degraded more than 5%.

As an example of solutions for air-handling units, virtual sensor of mixed air temperature by Yang and Li can be mentioned. [12] Mixed Air Temperature (MAT) is a useful measurement for control and diagnostics for economizers and vapor compression cycles. However, it can be very difficult to accurately measure MAT because of space constraints and the use of small chambers for mixing outdoor and return air in packaged ACUs. As inputs of VS were used: damper position signals, outdoor air temperature, return air temperature, and a calibrated virtual outdoor air ratio sensor. Both laboratory and field testing data were used to demonstrate an uncertainty of $\pm 1.0^{\circ}\text{F}$ (0.6K).

Virtual sensors for ACU sensible and total cooling capacity proposed by Yang and Li is based on manufacturers rating data. [2] The model covers all the operating conditions of the cooling system and overall tested predictions of cooling capacity are within 10%

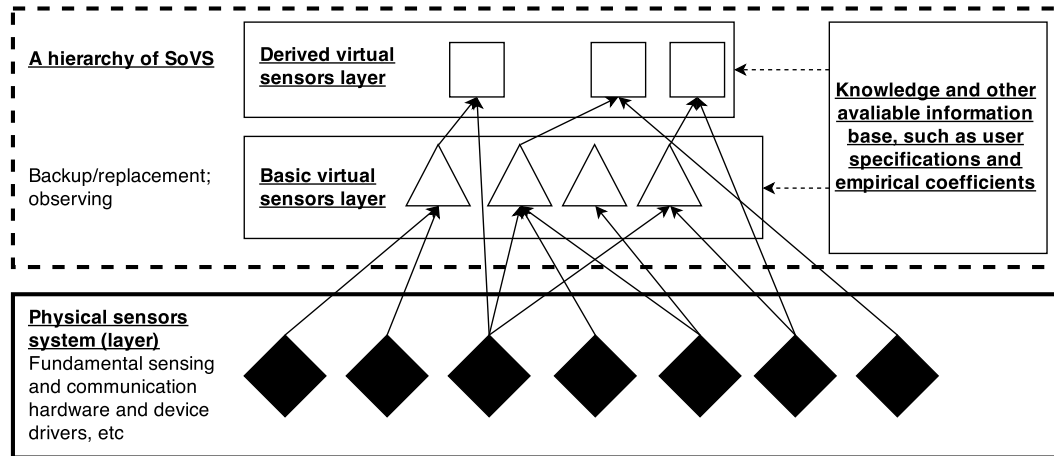


Figure 3 Systemization of virtual sensors [2].

Although this model requires four measurements (evaporator entering wet-bulb temperature, evaporator entering dry-bulb temperature, ambient temperature, and supply airflow rate) and not all of them can be measured by low-cost sensors commonly installed on AHUs.

Speaking of possible strategies to improve and expand virtual sensing technology in buildings, Li suggests idea of **systemization of virtual sensors (SoVS)**. Two classes of virtual sensor are proposed: basic and derived virtual sensors (Fig. 3). Basic virtual sensors are created using information from a group of physical sensors, empirical coefficients, and user specifications. They can be viewed as extensions of physical sensors that can be used as low-cost replacements or backups for physical sensors or to estimate quantities that cannot physically be measured. Conversely, a derived virtual sensor is a sensor model built from a combination of physical, basic, and/or other derived virtual sensor measurements. They could be used to provide higher level system information for performance monitoring, fault identification, and advanced control.

2.3 Existing solutions of virtual airflow sensor for AHU

D.Yu, H. Li, M. Yang proposed in their work method for virtual supply airflow rate meter for rooftop air-conditioning units which uses first-principle model in combination with accurate measurements of low-cost virtual or virtually calibrated temperature sensors. [4] Named disadvantages of physical airflow measuring and monitoring devices (PAFMs) are fragility, expensiveness, additional pressure loss and difficulties in installation. Mathematical model implemented in VS is based on simple energy balance equation:

$$\dot{V} = \frac{\dot{Q}_{sens}}{c_p \times |SAT - MAT|} \cdot \nu \quad (1)$$

where \dot{V} - volumetric air flow rate (m^3/s), \dot{Q}_{sens} - sensible capacity (kJ/s), SAT - supply air temperature ($^{\circ}C$), MAT - mixed air temperature ($^{\circ}C$), c_p - specific heat of the fluid ($J/(kg \cdot K)$), and ν is specific volume (m^3/kg). Since two opposite energy transmissions coexists in rooftop packaged unit (RTU), there are two approaches (cooling mode-based and heating mode-based approaches) to obtain the sensible capacity in Eq. (1).

Cooling-based model can be simplified to Eq. (2).

$$\dot{Q}_{C,sens} = \dot{Q}_C \times SHR = f(OAT, MAT, MAT_{wb}, \dot{V}_C) \quad (2)$$

where SHR is sensible heat ratio, \dot{V}_C is supply airflow rate in cooling mode (m^3/s), \dot{Q}_C is the gross cooling capacity (kJ/s), MAT_{wb} is critical point of the mixed air wet bulb temperature ($^{\circ}C$). By combining Eq. (1) and Eq. (2), the cooling-based approach formulation for a virtual flow rate meter can be expressed as:

$$\dot{V}_{C,model} = f(OAT, MAT, MAT_{wb}, SAT, \Delta T_{fan}) \quad (3)$$

where ΔT_{fan} - supply fan temperature rise ($^{\circ}C$). Accordingly, to develop a cooling-based flow rate meter, four dry bulb temperatures (OAT, MAT, SAT, ΔT_{fan}) and one wet bulb temperature (MAT_{wb}) was used, three of which (MAT, MAT_{wb} , ΔT_{fan}) were measured indirectly with virtual sensors.

In heating mode, gas burnt in furnace transmits heat into conditioned air and causes air temperature to increase so that process generally does not have mass transfer involved across the furnace. The measurement of conditioned air energy change relies purely on the air dry bulb temperature (Eq.4).

$$\dot{V}_{H,model} = f(\dot{V}_g, MAT, SAT, \Delta T_{fan}) \quad (4)$$

where \dot{V}_g is flue gas flow rate (m^3/s). Physical supply air temperature meter was used, although due to insufficient accuracy it was virtually calibrated utilizing statistical and modeling methods.

Both approaches were experimentally evaluated during laboratory tests. It was concluded that heating-based method is considerably more reliable and robust with uncertainty of 6.9% against 13.8% for cooling-based approach. Such high efficiency of this method ensues from utilization of furnace-type heater, which is also main disadvantage of the approach though, since in Europe water heaters are more common. Generally, process of development a flow rate meter is shown in Fig.4.

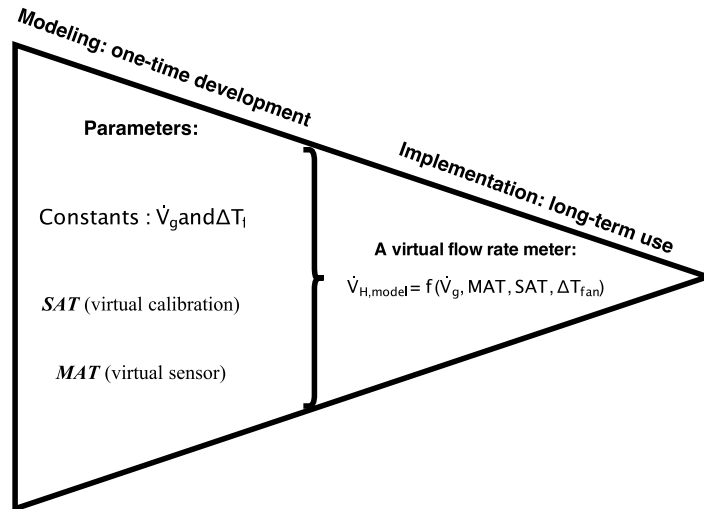


Figure 4 A scheme of deployment a virtual flow rate meter. [4]

In conclusion authors suggest to utilize this VS for serving as part of permanently installed control or monitoring system to indicate the real-time flow rate, automatically detect and diagnose improper readings, detecting RTU air side faults such as dirty indoor filters and slipping supply fan belt.

2.4 Summary

Virtual sensors are not only cheaper alternative to physical ones: in many cases such solutions provides even more reliable and accurate measurements (mixed air temperature in AHU, air flows). This features of VSs makes them very useful tool in creating cost-effective fault detecting systems capable of diagnosing wider range of failures.

Since there is still lack of reliable solutions of airflow rate VSs for AHU systems, especially for European conditions, new alternative method will be proposed in this paper.

3 Theoretical basis and Virtual Sensor design

In this chapter main physical equations will be derived, likewise basic information about heat recovery ventilators and AHU will be given, also Simulink[®] models of virtual sensor will be described.

3.1 General information

Virtual sensor will be developed as mathematical model, derived from heat balance for heat recovery ventilator. Heat recovery ventilator (HRV) is air-to-air heat exchanger which employs heat exchange between the inbound and outbound air flow. HRV provides fresh air and improved climate control, while also saving energy by reducing heating (and cooling) requirements. [13] Over last two decades HRV moved from experimental and uncommon equipment to almost compulsory part of HVAC systems for commercial buildings, so VS based on it can be easily implemented in majority of modern installations. [14] Most common type of HRV is recuperator. Such devices

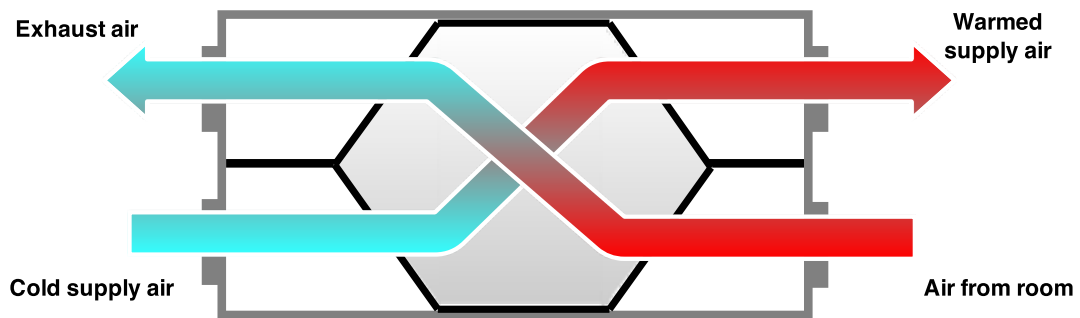


Figure 5 Generic scheme of recuperator (winter mode).

typically comprise a series of parallel plates of aluminum, plastic, stainless steel, or synthetic fiber, alternate pairs of which are enclosed on two sides to form twin sets of ducts at right angles to each other, and which contain the supply and exhaust air streams. Normally the heat transfer between air streams provided by the device is termed as 'sensible', which is the exchange of energy, or enthalpy, resulting in a change in temperature of the medium (air in this case), but with no change in moisture content. [13]

Heat flux between two fluids inside heat exchanger can be estimated with temperature measurements and depends on exchanger type, geometry, parameters of fluid

(that for air depend mostly on temperature) and mass flow rate. That fact makes possible to estimate air mass flow rate from temperature measurements and knowledge of recuperator parameters.

Main advantages of this method are:

- It is based on simple physical principles, so no sophisticated model training is required.
- Uses only temperature sensors, which are standard equipment of modern AHUs
- Model is built mostly on basic arithmetical operations, so it can be run on simple SoC, PLC or even directly on AHU's control unit.
- It has potentially wide range of commercial application, since HRV is a common part of ventilation system
- Majority of recuperators has consimilar construction, that simplifies sensor implementation.
- Heat exchanger itself has no mechanical parts and is protected from both sides by filters, so its qualities are practically stable along all life-cycle of system.
- Method can be used in both winter and summer periods.

Disadvantages of method will be studied during laboratory tests.

Recuperator parameters can be expressed in two ways: as so-called performance curves or as exchanger type, geometry and used material. According to that, two respective approaches of mass flow rate calculation are proposed.

Both approaches require four temperature measurements:

- t_s - temperature of supply air in front of HRV
- t'_s - temperature of supply air behind HRV
- t_e - temperature of exhaust air in front of HRV
- t'_e - temperature of exhaust air behind HRV

3.2 Performance curves approach

Temperature Transfer Efficiency (TTE) is most commonly used parameter defining ability of HRV to transfer heat from hotter air to colder. It depends on physical parameters of HRV, air flow rates and humidity. [15] It can be expressed with performance curves, which is empirically established dependency $TTE = f(\dot{V})$, where \dot{V} is volumetric air flow rate inside recuperator (m^3/h). It is usually provided by manufacturer of AHU as part of technical documentation in form of graph.

Although, strictly speaking, performance curve is only applicable for case of equal flow rates in both supply and exhaust directions. Also in case when air temperatures differ from laboratory conditions correction for thermal density change should be made. Generally:

$$TTE = f(\dot{C}_{min}) \quad (5)$$

where \dot{C} - heat capacity rate of the fluid (W/K), \dot{C}_{min} - lower value of \dot{C}_s and \dot{C}_e , index s states for supply flow, e - for exhaust flow. The heat capacity rate denoting the quantity of heat a flowing fluid of a certain mass flow rate is able to absorb or release per unit temperature change per unit time: [15]

$$\dot{C} = c_p \dot{m} \quad (6)$$

where c_p - specific heat of the fluid (J/(kg*K)), \dot{m} - mass flow rate of the fluid of interest (kg/s).

$$TTE = \vartheta_s \frac{\dot{C}_s}{\dot{C}_{min}} = \vartheta_e \frac{\dot{C}_e}{\dot{C}_{min}} = \vartheta_{max} \quad (7)$$

where ϑ_{max} - higher value of ϑ_s and ϑ_e , ϑ - temperature ratio calculates as:

$$\begin{aligned} \vartheta_s &= \frac{t'_s - t_s}{t_e - t_s}, \\ \vartheta_e &= \frac{t_e - t'_e}{t_e - t_s} \end{aligned} \quad (8)$$

For air c_p is constant for wide range of temperatures, that simplifies eq. 7 to:

$$TTE = \vartheta_s \frac{\dot{m}_s}{\dot{m}_{min}} = \vartheta_e \frac{\dot{m}_e}{\dot{m}_{min}} = \vartheta_{max} \quad (9)$$

For $\vartheta_s \geq \vartheta_e$ ($\dot{m}_s \leq \dot{m}_e$) this equation has solution:

$$\begin{aligned} \dot{m}_s &= \frac{1}{f}(TTE), \\ \dot{m}_e &= \dot{m}_s \frac{\vartheta_s}{\vartheta_e}, \end{aligned} \quad (10)$$

For $\vartheta_e > \vartheta_s$ ($\dot{m}_e < \dot{m}_s$):

$$\begin{aligned} \dot{m}_e &= \frac{1}{f}(TTE), \\ \dot{m}_s &= \dot{m}_e \frac{\vartheta_e}{\vartheta_s}, \end{aligned} \quad (11)$$

For purposes of this research function f will be represented in polynomial form, though it can also be a table.

3.2.1 Construction of the model in Simulink[®] software

Eq. 10 and 11. were converted to Simulink[®] computing model as it shown on fig.6

As can be seen on fig.6 outputs of the model are two mass air flow rates, although in literature and standards concept of volumetric flow rate is more common. Decision to operate with mass flow instead of volumetric flow was made because, generally speaking, since volume air flow depends on density, which in turn depends on temperature and other factors, it will be different in each point of ventilation system. This problem causes obstacle for evaluation of Virtual Sensor using physical meters, which placed at a distance from HRV. Whereas mass air flow rate could be constant along AHU, assuming that system is airtight. Obviously, mass air flow rates can be subsequently converted to volumetric ones with certain accuracy.

3.3 Recuperator geometry approach

Energy exchange process in recuperator can be described as heat transfer between two flowing fluids through flat plate. Mathematical model of this process will be derived from known physical relations, also some simplifications will be made:

1. Recuperator will be represented as single plate of square equivalent to heat transfer surface.

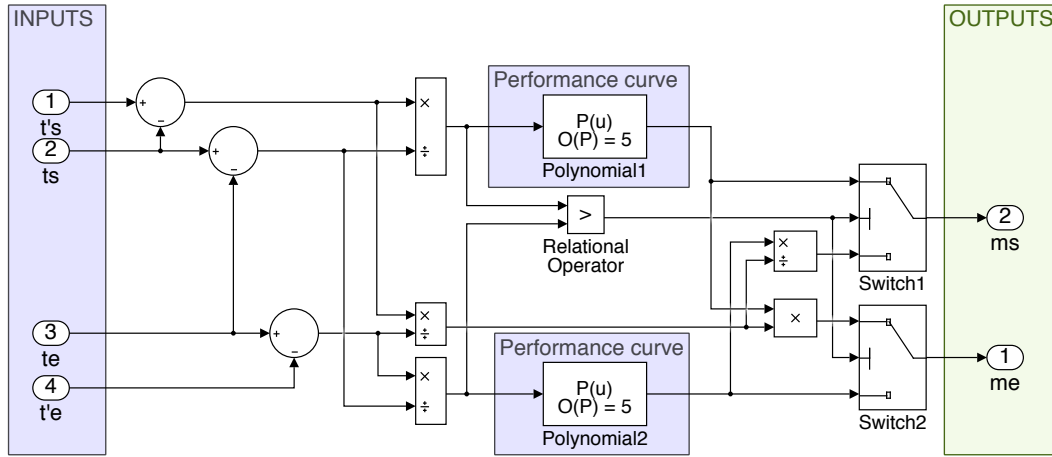


Figure 6 Diagram of Virtual Sensor - Performance curves approach

2. Flow arrangement is counter-current
3. Heat losses will be neglected.
4. Heat transfer process is steady.

Since process can be considered as quasi-static, in every moment of time \dot{Q} amount of heat is transferred between \dot{m}_s of supply air and \dot{m}_e of exhaust air. As a result temperatures of supply and exhaust air will change respectively from t_s to t'_s and from t_e to t'_e . Heat received (lost) by matter causes change in temperature of this matter according to heat equation:

$$\dot{Q} = \dot{m}c_p\Delta T \quad (12)$$

where \dot{Q} is transferred heat (W), ΔT is the change in temperature (K). On the other

hand, heat transfer between two fluids in counter-current heat exchanger (convection-conduction-convection mechanism) is [15]

$$\dot{Q}' = b\Delta T_m \quad (13)$$

where ΔT_m - logarithmic mean temperature difference (LMTD):

$$\Delta T_m = \frac{(t_e - t'_s) - (t'_e - t_s)}{\ln\left(\frac{t_e - t'_s}{t'_e - t_s}\right)} \quad (14)$$

and

$$b = \frac{S}{\frac{1}{h_s} + \frac{\delta}{\lambda_p} + \frac{1}{h_e}} \quad (15)$$

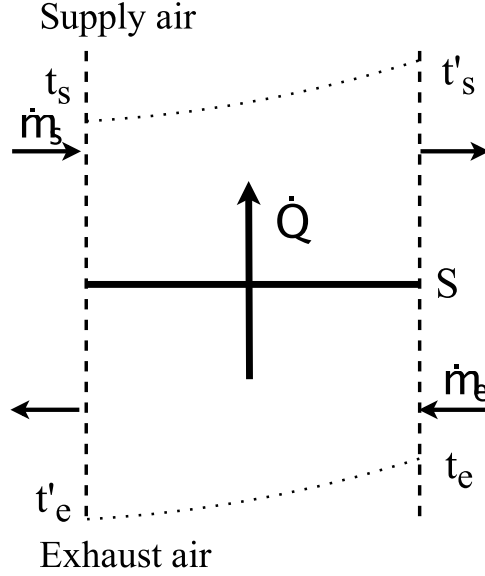


Figure 7 Heat exchange process in recuperator.

where δ_p - thickness of plate (m), λ_p - thermal conductivity of plate ($Wm^{-1}K^{-1}$), h_s and h_e - heat transfer coefficients resp. on supply and exhaust sides of plates ($W/(m^2K)$), S - equivalent heat transfer surface (m^2).

As was stated at the beginning of this chapter, equations will be derived for counter-current arrangement of flows. For cross-current heat exchangers LMTD should be corrected with coefficient F :

$$\Delta T_{m,corr} = F \Delta T_m \quad (16)$$

Where coefficient $F < 1$ depends on type of exchanger and flow rates ratio. [15]

Heat transfer coefficients depend on flow regime, characteristics of fluid, plate dimensions and in case of airflow around the plate can be described as:

$$h = \frac{Nu \lambda_f}{L} \quad (17)$$

where Nu is Nusselt number - dimensionless average heat transfer rate, λ_f - thermal conductivity of fluid ($Wm^{-1}K^{-1}$), L - characteristic linear dimension (m), which in case of rectangular duct calculates as hydraulic diameter:

$$L = D_h = \frac{2ah}{a+h} \quad (18)$$

For forced convection, the Nusselt number is generally a function of the Reynolds number and the Prandtl number. Exact form of equation is geometry specific and derived empirically for each case. [5]

Average Nusselt number for forced convection over a flat plate for laminar regime:

$$Nu^* = 0.664 Re^{0.5} Pr^{1/3} \quad (19)$$

for turbulent flow:

$$Nu^* = 0.035 Re^{0.8} Pr^{1/3} \quad (20)$$

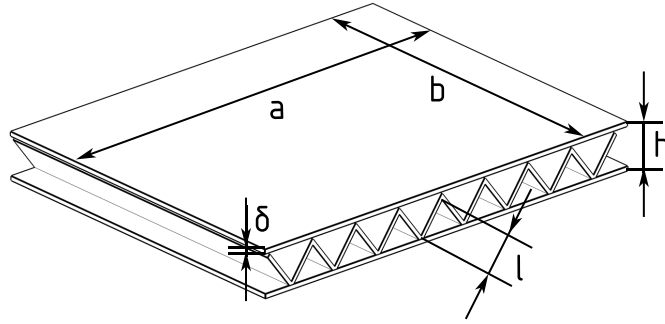


Figure 8 Plate geometry

where Re - Reynolds number and Pr - Prandtl number:

$$Re = \frac{uL}{\nu} \quad (21)$$

$$Pr = \frac{\nu}{\alpha} \quad (22)$$

u - velocity of flow (m/s), ν - kinematic viscosity of the fluid (m^2/s), α - thermal diffusivity of fluid (m^2/s),

Mean flow velocity (u) inside recuperator can be calculated from mass flow rate \dot{m} with equation:

$$\dot{u} = \frac{\dot{m}}{nS_c\rho} = \frac{\dot{m}}{n \cdot a \cdot h \cdot \rho} \quad (23)$$

where S_c - area of a single channel between two plates (m^2), ρ - air density (kg/m^3), n - number of channels.

Since plates of HRV are usually equipped with fins, correction for fins efficiency (η) should be made:

$$Nu = \eta Nu^* \quad (24)$$

Equation for triangular fins efficiency: [5]

$$\eta = \frac{\tanh \sqrt{0.5 Nu^* \frac{\lambda_f}{\lambda_p} \frac{l}{D_h} \frac{l}{\delta} (\frac{\delta}{b} + 1)}}{\sqrt{0.5 Nu^* \frac{\lambda_f}{\lambda_p} \frac{l}{D_h} \frac{l}{\delta} (\frac{\delta}{b} + 1)}} \quad (25)$$

where b, l, δ - dimensions of plate according to fig.8.

As mentioned before, heat losses would be neglected, so all heat lost by hotter airflow will be received by colder one, from assumption that supply air is colder:

$$\dot{Q}_s = \dot{Q}_e = \dot{Q}' \quad (26)$$

$$\dot{m}_s \cdot c_{ps}(t'_s - t_s) = \dot{m}_e \cdot c_{pe}(t_e - t'_e) = b\Delta T_m \quad (27)$$

Consequently, mass flow of supply air is:

$$\dot{m}_s = \frac{\Delta T_m}{t'_s - t_s} \cdot \frac{b}{c_{ps}} \quad (28)$$

and mass flow of exhaust air is:

$$\dot{m}_e = \frac{\Delta T_m}{t'_e - t_e} \cdot \frac{b}{c_{pe}} \quad (29)$$

Comments:

1. There are some quantities in equations above dependent on temperature, such as ρ, λ, ν, c_p . Those values are estimated for mean temperature inside recuperator.
2. Condensation or frost inside recuperator dramatically change heat transfer process so used dependencies are no longer applicable. Taking into account this state would significantly complicate calculations, besides with properly operating anti-freeze protection and average humidity of indoor air those states should not occur during AHU functioning. That fact makes doubtful financial effort of such extended models.
3. Also those quantities are dependent on air pressure and humidity. This dependency will be neglected due to lack of respective sensors in commercial AHUs, besides impact of pressure and humidity is considerably lower than impact of temperature and should not significantly affect the results.
4. Derived physical principles are applicable only for stable state: successful modeling of transient processes requires very accurate input data measurements, on the other hand, taking into account dynamics dramatically increases complexity of method.

3.3.1 Construction of the model in Simulink® software

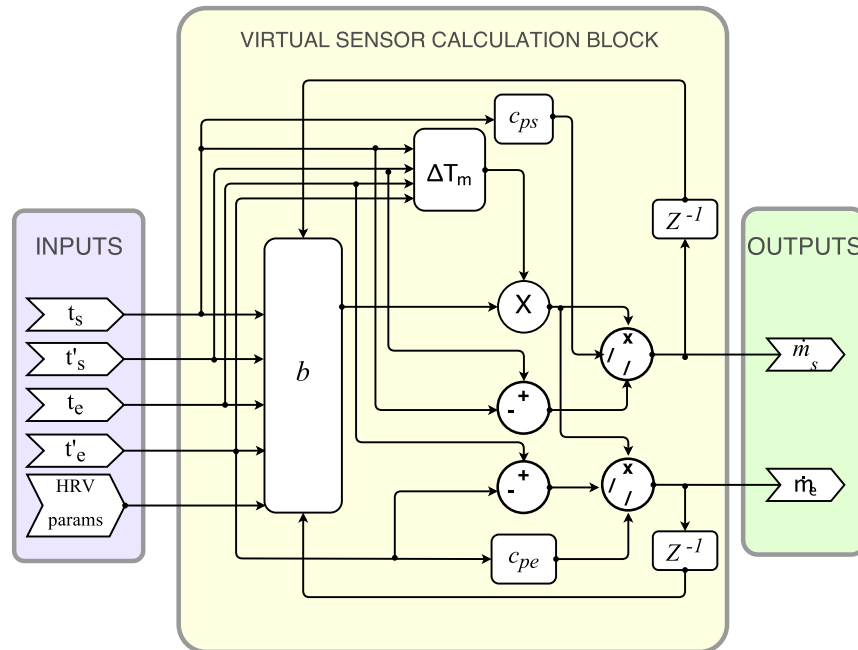


Figure 9 Simplified diagram of Virtual Sensor - Recuperator geometry approach

Simulink® computing model was created according to eq. 28 and 29. Model consists of five main function blocks (fig.9):

- **Coefficient b calculation block:** represents eq. 15, also calculates density of exhaust and supply air depending on measured temperature. Containing all used HRV parameters specific for exact unit.
- **Logarithmic temperature difference calculation block:** represents eq. 14.
- **Heat transfer coefficient calculation block** (*not presented on diagram*): According to Reynolds's number estimates flow regime (laminar or turbulent).
- Supply and exhaust air parameters (such as ***heat capacity, density, kinematic viscosity and thermal conductivity***) were estimated depending on temperature measurements using 1-D look-up referential tables. Influence of pressure, humidity and other factors was neglected.
- Coefficient b contains heat transfer coefficients, which in turn depends on mass flow. To solve this loop function blocks of one-step delay was used. (\mathbf{Z}^{-1} on diagram)

Overall Simulink diagram of Virtual sensor is shown in Appendix A.

4 Evaluation of Virtual Sensor with Laboratory tests

In this chapter results of laboratory tests of Virtual Sensor on AHU test rig will be presented.

4.1 Test rig configuration and parameters

AHU testing rig was designed by Vladimir Horyna and Ondrej Hanus for the purpose of performance monitoring and FDD development. From technological perspective test rig mimics typical commercial solutions: basic functional nodes (heater, cooler, recuperator, fans, filters), communication ducts and materials are similar to those, which are widely presented on market and commonly used by manufacturers. Conversely, measuring system is more complicated and consists of broad set of sensors, rarely used in field. Such system allows identify conditions in several critical points across the AHU. The basic unit of measuring system is IN CompactRIO 9081. It is fully-fledged industrial computer with ability to connect different measuring modules, which collects processes and stores all measured data. [16]

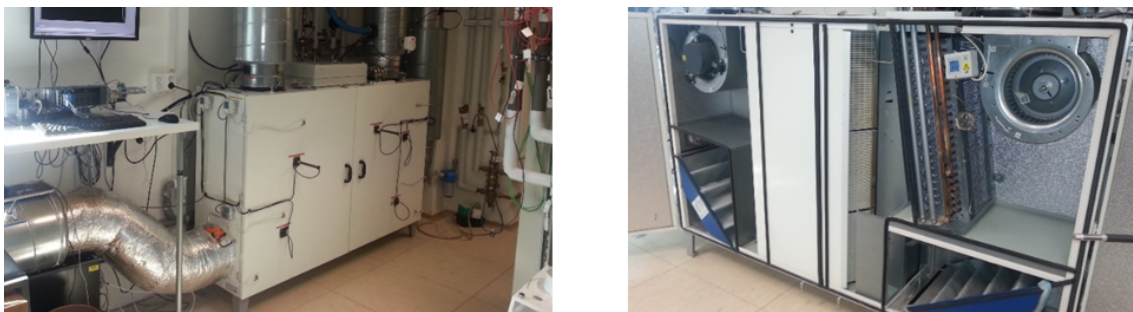


Figure 10 AHU testing rig

HVAC unit is connected to a special testing chamber where various conditions can be set thanks to possibility to heat or cool each wall separately. On the HVAC system a lot of disturbances typical for HVAC units (like clogged filter etc.) can be simulated.

4.1.1 Installed sensors

1. Air velocity sensors:

- **Type:** vane wheel insertion probes by the brand Hontzsch
- **Range:** 0-20m/s

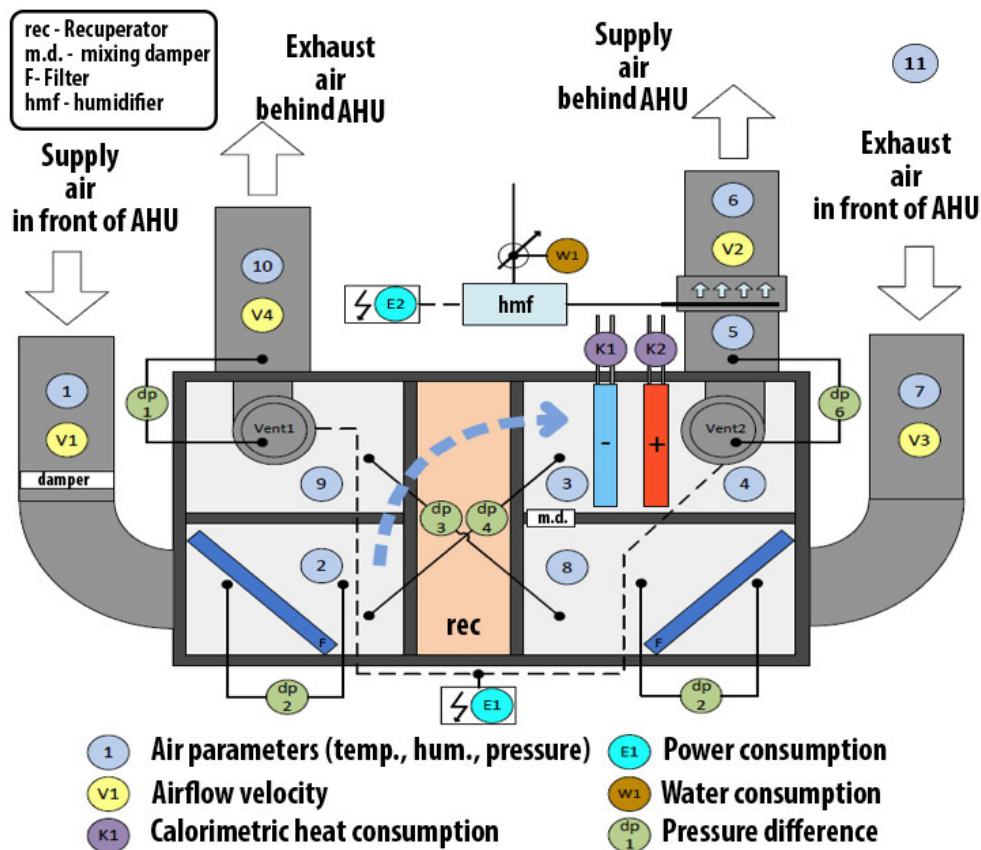


Figure 11 Block arrangement of AHU test rig. [16]

- **Uncertainty:** not more than 1.5% of measured value and +0.5% of full range.
- 2. Multi-functional (temperature and air conditions) sensors:
 - **Type:** Vaisala HMP110 (thermistor Pt1000)
 - **Range(temperature):** 0 to 40°C , -40 to +80°C
 - **Uncertainty(temperature):** ±0,2°C, ±0,4°C.
- 3. Power consumption meter:
 - *Not used in tests*
- 4. Water consumption meter
 - *Not used in tests*
- 5. Calorimetric heat consumption meter
 - *Not used in tests*
- 6. Pressure difference
 - *Not used in tests*

During laboratory tests outputs of Virtual Sensor were compared to readings from V1 (Supply Air) and V4 (Exhaust Air) anemometers. Measuring system provides real time calculation of volumetric airflow from flow velocity measurements.

Necessary temperatures measurements were obtained from multi-functional sensors:

- Sensor 2 - Supply air – in front of recuperator
- Sensor 3 - Supply air – behind recuperator
- Sensor 8 - Exhaust air – in front of recuperator
- Sensor 9 - Exhaust air – behind recuperator

All measurements were conducted with sampling rate of 12s for long-term experiments and 2s for short-term experiments.

4.1.2 Parameters of heat exchanger

- **Equivalent heat transfer surface:** $98m^2$
- **Single gap dimensions (see fig.8):**
 - $a=0.30m$
 - $b=0.50m$
 - $h=0.004m$
 - $\delta=0.001m$
 - $l=0.006m$
- **Number of gaps (in one direction):** 122
- **Thermal conductivity of plate:** $16Wm^{-1}K^{-1}$ (High impact polystyrene)

4.1.3 Performance curve measurement

Data for performance curve construction were gained from all experiments described in this chapter.

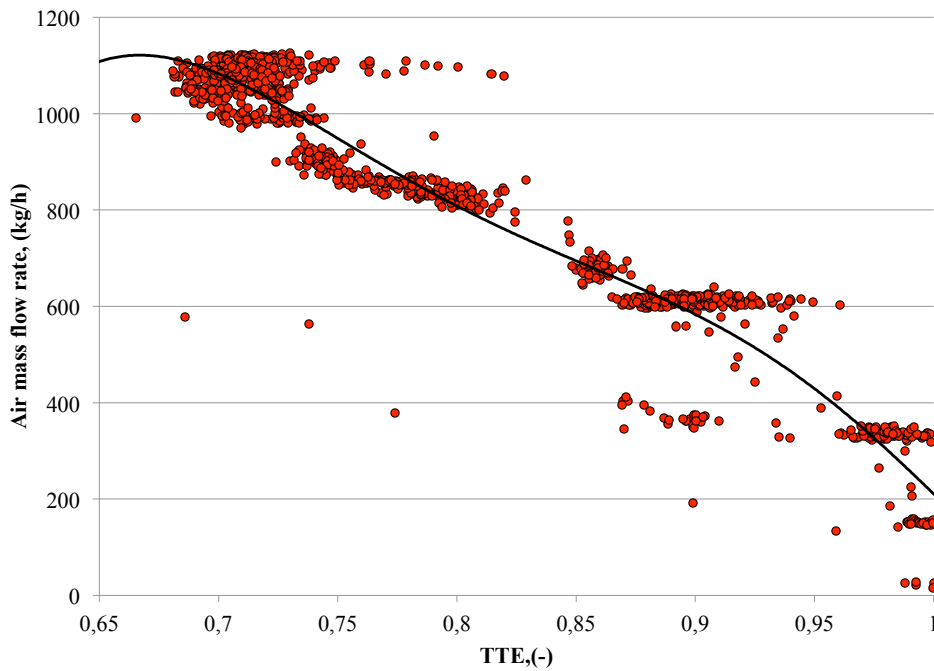


Figure 12 Performance curve of test rig

Trend line of scatter can be described with polynomial equation:

$$\dot{m} = (-1,594TTE^5 + 5,330TTE^4 - 6,623TTE^3 + 3,578TTE^2 - 0,690TTE) \cdot 10^5 \quad (30)$$

4.2 Data processing

Generally, volumetric airflow is different in every point across the duct because of fluctuations of air density caused by temperature changes. Due to that fact, as a first step of data processing, volumetric-to-mass flow conversion was made. Measurements of local air density was provided by multi-functional sensors 6 and 1 (fig.11).

Multi-functional sensors were placed in front of and behind HRV. Average between those pairs of temperatures were used to estimate density and other air parameters inside recuperator. All measured values were additionally processed with Simple Moving

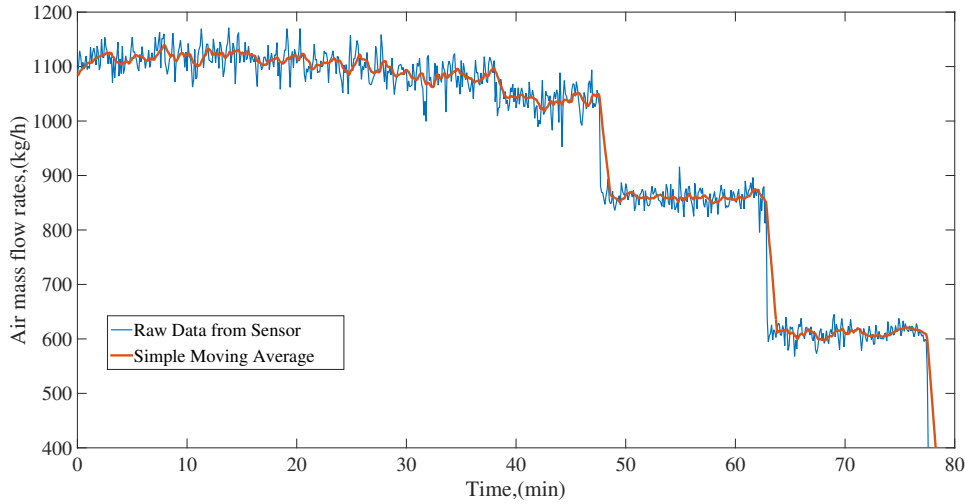


Figure 13 Input data filtration (Exhaust air)

Average (SMA) filter to reduce noise caused by strong random airflow turbulences and rapid environment changes.

4.3 Transient state correction

As was mentioned in chapter 3, models provide reliable outputs only when system is in steady-state. Although temperatures inside recuperator have relatively long settling time (5 to 20 minutes depending on conditions), when model potentially could lost its accuracy. That prediction was approved with laboratory test (see fig.14): during that test inlet damper position have been changed every 10-15min, which caused step-like flow changes of supply air.

To improve dynamic qualities of performance curve model, equation 8 where corrected in following way:

$$\begin{aligned} \vartheta'_s &= \vartheta_s \cdot \left(1 + k_1 \frac{d\vartheta_s}{dt}\right), \\ \vartheta'_e &= \vartheta_e \cdot \left(1 + k_2 \frac{d\vartheta_e}{dt}\right) \end{aligned} \quad (31)$$

where ϑ'_s , ϑ'_e - corrected values of ϑ_s and ϑ_e , k_1 and k_2 - gain coefficients estimated empirically.

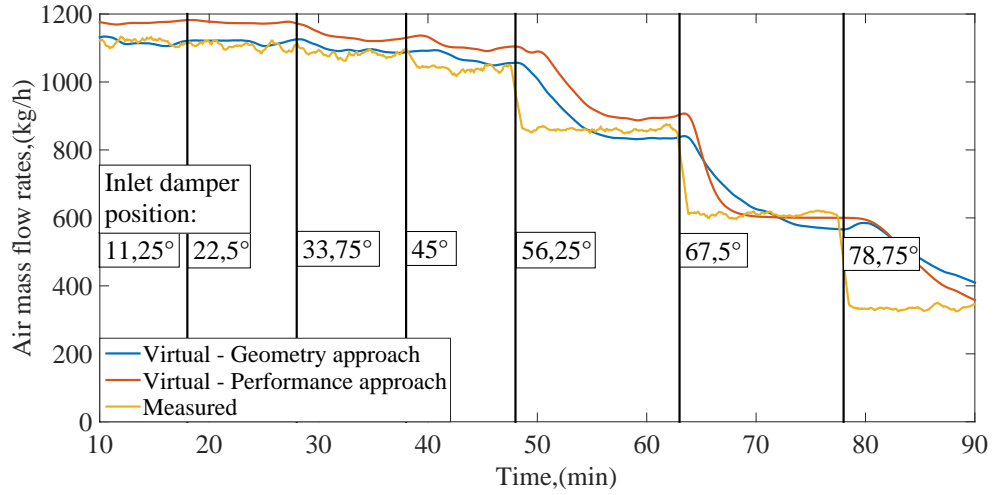


Figure 14 Supply mass airflow temperature settling

Respectively, corrected equations 28 and 29 for geometry approach model:

$$\dot{m}'_s = \dot{m}_s \cdot \left(1 + k_3 \frac{d(\vartheta_e/\vartheta_s)}{dt}\right) \quad (32)$$

$$\dot{m}'_e = \dot{m}_s \cdot \left(1 + k_4 \frac{d(\vartheta_e/\vartheta_s)}{dt}\right) \quad (33)$$

where \dot{m}'_s , \dot{m}'_e - corrected values of air flow rates, k_3 and k_4 - gain coefficients estimated empirically.

Models were changed according to corrected equations. Additionally outputs from all derivations were filtered with Simple Moving Average. Results of tests with corrected models are presented at fig.15

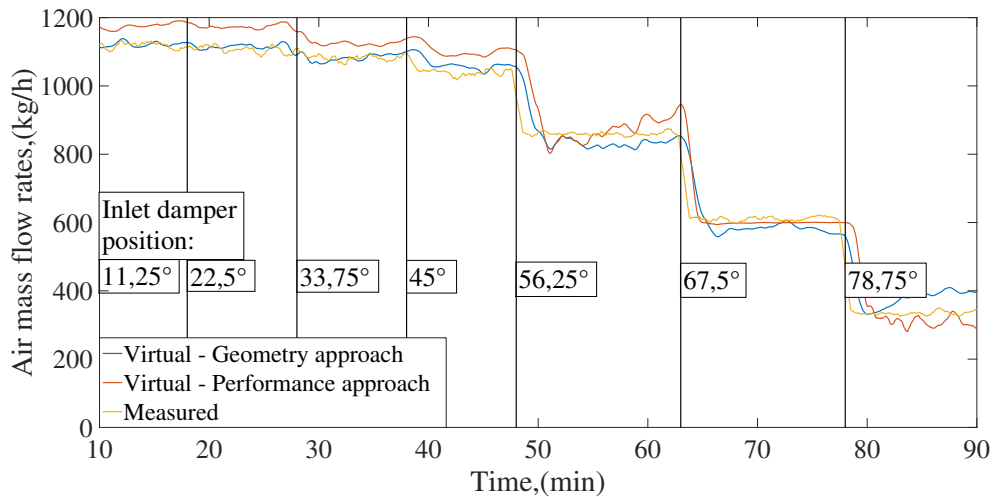


Figure 15 Supply mass airflow transient states corrected

All further testing will be conducted with corrected models, as they provide clearly more accurate estimation in rapidly changing conditions.

4.4 Laboratory tests results

4.4.1 Long-term experiments

First series of tests were conducted from 20.02.2015 till 10.03.2015. Aims of this test were to examine and compare precision of models in conditions close to field ones and estimate possible weaknesses of method for further testing. Before experiments started

AHU had been set up with following settings:

- **Exhaust fan speed:** Maximum
- **Supply fan speed:** Maximum
- **By-pass damper:** closed
- **Circulation damper:** closed
- **Temperature inside room (set-point):** 32°C .

Those parameters have been changed several times during experiment: fan speeds have been set to different values (firstly for both exhaust and supply fans, then independently); temperature inside room have been gradually decreased till heating turned off completely. Once AHU was shut down completely for approximately two hours, due to problems with power supply.(see fig.17)

Conditions during experiment were:

- **Temperature outside (daytime):** $+6.5 \sim +16.5^{\circ}\text{C}$
- **Temperature outside (nighttime):** $-2.0 \sim +3.5^{\circ}\text{C}$
- **Humidity outside:** $25 \sim 87\%$
- **Humidity in room:** $11 \sim 31\%$

Temperature curves for this experiment are presented on fig.16

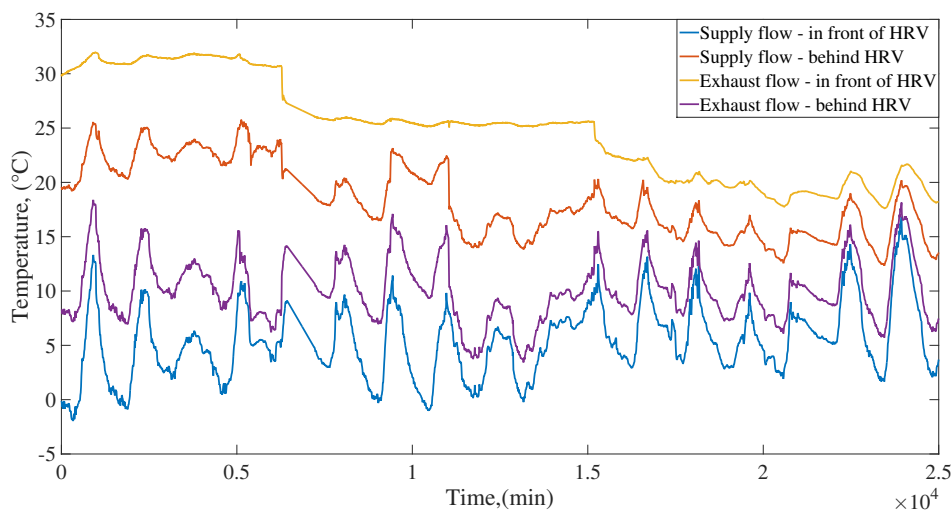


Figure 16 Temperature readings - experiment 20.02.2015-10.03.2015

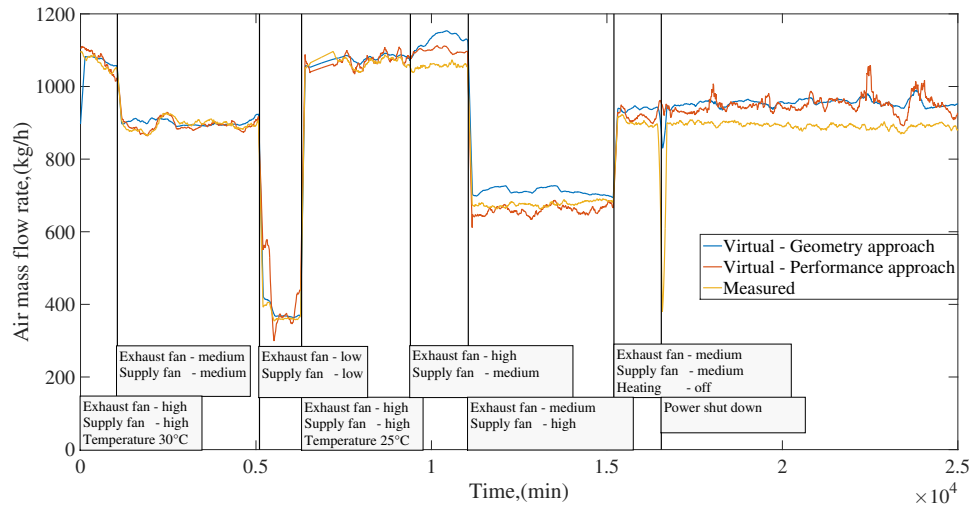


Figure 17 Exhaust mass airflows - experiment 20.02.2015-10.03.2015

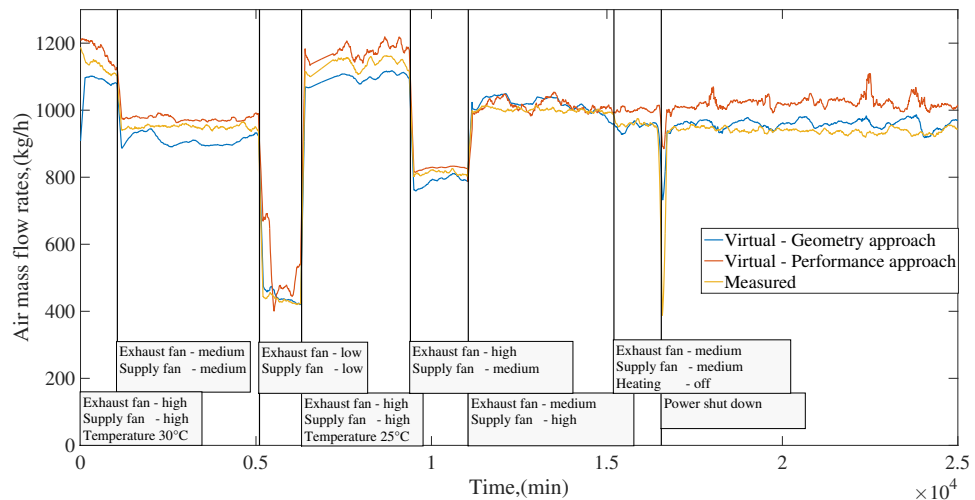


Figure 18 Supply mass airflows - experiment 20.02.2015-10.03.2015

Virtual sensors demonstrated uncertainty:

For exhaust air flow

performance curve approach: $\pm 56 \text{ kg/h}$ ($\pm 7.57\%$ of full range);

geometry approach: $\pm 55 \text{ kg/h}$ ($\pm 7.45\%$);

For supply air flow

performance curve approach: $\pm 69 \text{ kg/h}$ ($\pm 8.67\%$);

geometry approach: $\pm 40 \text{ kg/h}$ ($\pm 4.98\%$).

Here should be mentioned that estimation of flow rate with anemometer has it's own uncertainty which might be high due to indirect character of measurement. According to this, presented numbers can not be deemed as trustworthy assessment and could be used only for approximate evaluation of sensor. For correct evaluation more precise sensor should be used, for instance thermal mass flow meter [17].

Model based on geometry approach has shown better results, especially for supply air, though results of both models were close to each other.

Moving force of heat exchange process in recuperator is temperature difference between two airflows, that fact allows to prognosticate decreasing precision of method as this difference gets closer to zero. That estimation has been approved during the test: precision of models noticeably worsened at the end of experiment after heating was turned off.

Also, due to small size of testing chamber against high mass rate of supply air, temperature in room destabilized and started replicate daily peaks of outside temperature. That caused noticeable oscillations in virtual sensors (both geometry and performance curves approaches) reading at the end of experiment. That problem can be dismissed with additional filtration, though it will also affect dynamics of model. In "field" conditions rooms have larger heat capacity, so such oscillations of temperature most likely will be muted.

Airflow rates have been changed from 400 to 1100 kg/h with fans speed adjustments. No significant change in model error correlating with flow rate have been discovered. Although, as can be seen on diagram, models are less precise when air flows are asymmetrical, especially for exhaust air. That correlation was studied closer during next experiment.

4.4.2 Short-term experiment 1 - high temperature difference

Test was conducted 13.04.2015 from 15:44 till 17:18. The main aim of this experiment was to establish usability range of airflow rates ratio and also examine dynamic qualities of models. During that test inlet damper has been gradually closed, simulating duct clogging. Damper position have been changed every 10-15min, which caused flow changes of supply air. Temperature difference between exhaust and supply air was within 10 to 20K range.

After models settled (10th min), for supply flow estimation error was stable (approx. 30kg/h for geometry approach and 70kg/h for performance approach) until damper position reached 78, 75° when for geometry approach it has grown to 70kg/h and then to 170kg/h for 90°

For exhaust flow both models have significant lost in accuracy starting from 78, 75° position. Also performance curve model overreacted at moments of damper position change.

According to experiment results, model of slower flow (in our case supply air) keeps usable precision till flow rates ratio reaches number of five, whereas for faster flow (exhaust) the critical ratio is 2.5 (damper is in 78, 75° position). Here should be mentioned that such big difference between supply and exhaust air can only come as a consequence of serious system failure, and rarely happens under normal conditions and although in that case model can not be used for precise flow rate estimation, failure itself is still recognizable from sensor readings.

For supply air model based on performance curve better corresponded with expected values.

4.4.3 Short-term experiment 2 - medium temperature difference

Test was conducted 13.04.2015 from 12:00 till 13:55. Temperature inside testing chamber was cooled down with outdoor air to 21°C. Aim of this experiment were to examine models performance in medium temperature difference conditions (5.5 to 7.5K). Test

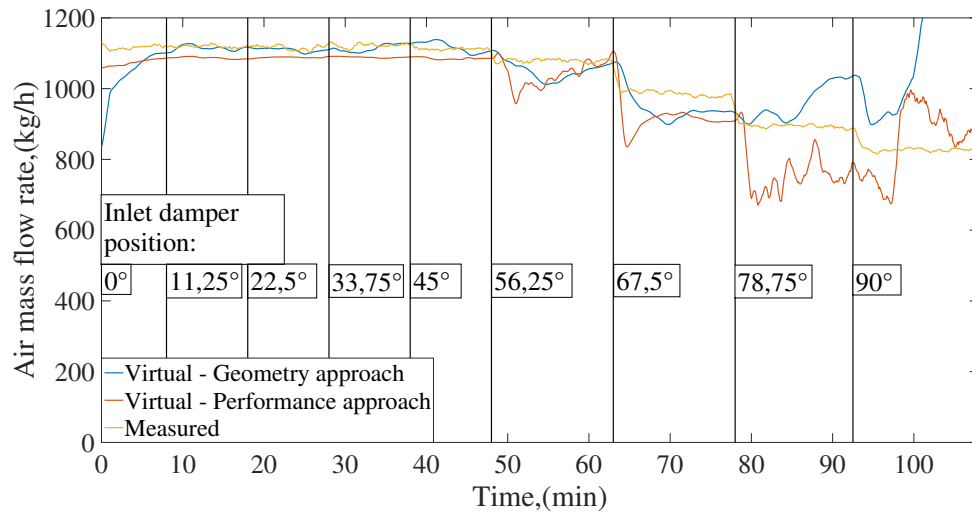


Figure 19 Exhaust mass airflows - experiment 1.04.2015

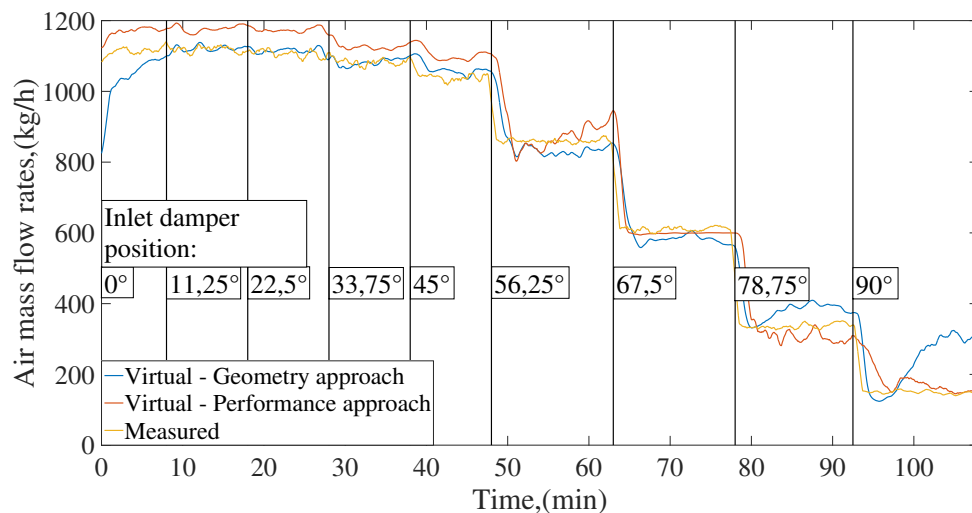


Figure 20 Supply mass airflows - experiment 1.04.2015

was conducted in a similar way as previous one. Comparing to previous experiment, both models have not shown significant signs of accuracy reduction: mentioned critical values of air flows ratio remained on the same level, though both signals became more noisy.

Errors of measurements were practically at the same level as for previous experiment. For performance approach model of supply flow error has grown to to 100kg/h for 90°, whereas in previous test it remained at lower level even for this damper position.

4.4.4 Short-term experiment 3 - low temperature difference

Test was conducted 5.05.2015 from 16:00 till 17:35. Aim of this experiment were to examine models performance in low temperature difference conditions (1 to 2K). Test was conducted in a similar way as previous one. Before experiment started temperature

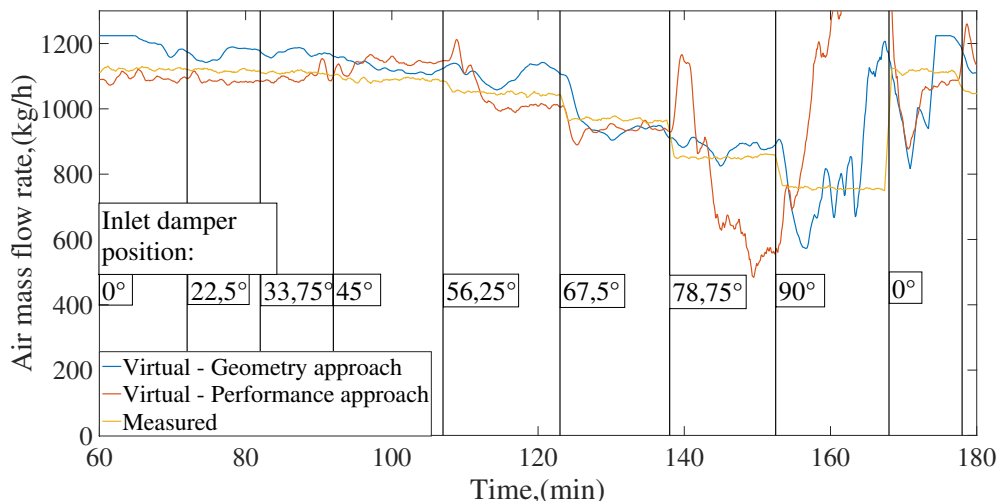


Figure 21 Exhaust mass airflows - experiment 13.04.2015

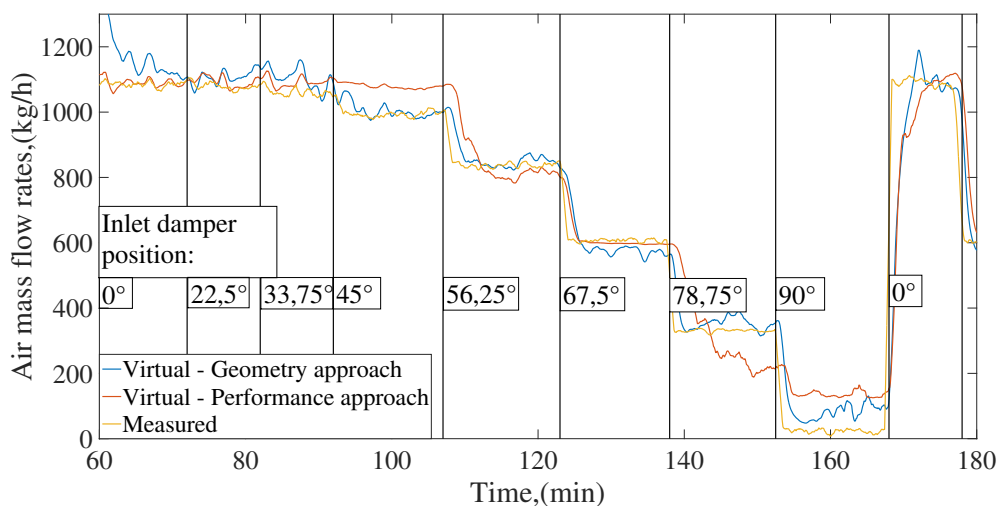


Figure 22 Supply mass airflows - experiment 13.04.2015

of outdoor air was close to $26^{\circ}C$ and temperature of indoor air was $26.5^{\circ}C$. To increase such extremely low temperature difference, heater has been turned on as experiment started, so temperature difference gradually increased from 0.5K to 1.8K. Original results show noticeable signs of noisiness growth, especially for geometry approach (see fig.23, 24)

To reduce noise additional filtration has been applied (fig.25, 26).

As can be seen on figures, models provide reliable results starting from 12th minute, when temperature difference reached 1.5K. Although, as it was expected, additional filtration worsened dynamics of VS, so exact moments of damper position change are not clearly readable from sensors outputs. For exhaust flow readings are reliable till it less than 1.7 times faster than supply flow.

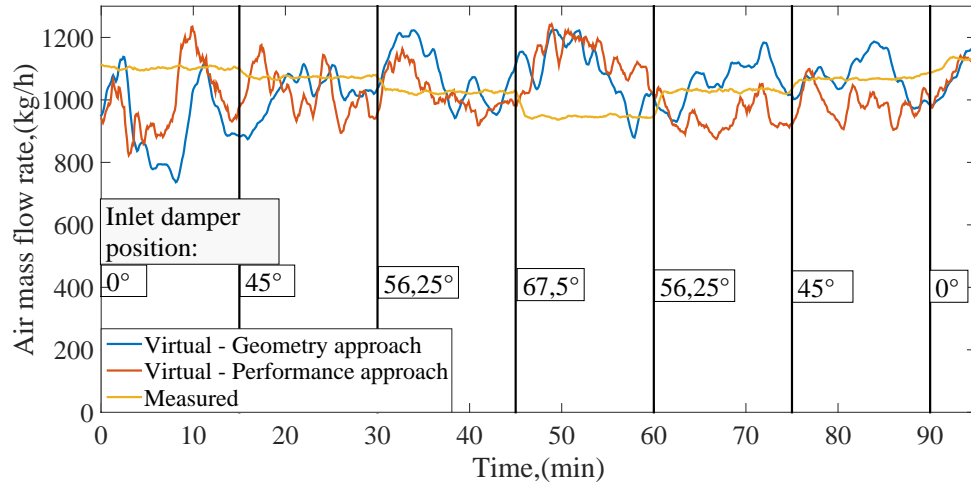


Figure 23 Exhaust mass airflows - experiment 5.05.2015

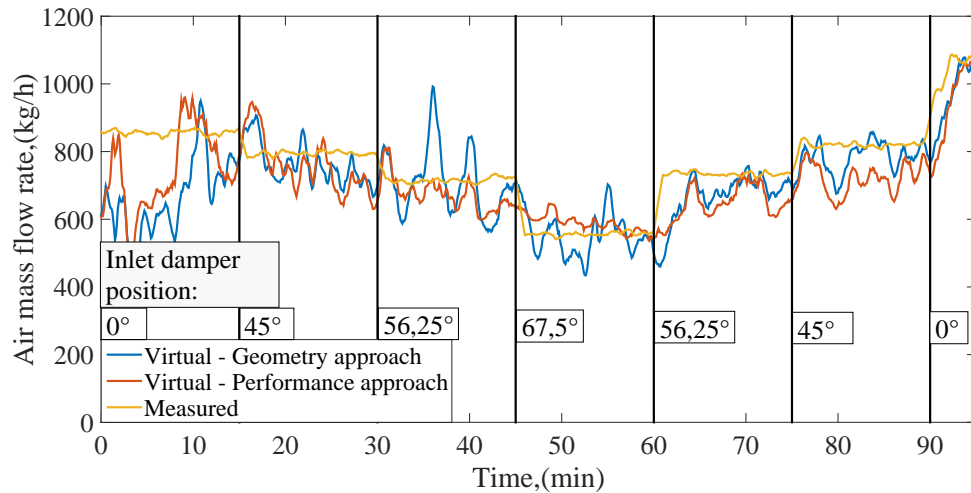


Figure 24 Supply mass airflows - experiment 5.05.2015

4.5 Usage of alternative thermometers positions

For all described experiments temperature sensors, used as inputs of model, were placed in close proximity to the heat exchanger. That sensors arrangement provides best results and minimizes errors in temperature measurements. On the other hand, commercial AHUs do not necessarily have the same sensors arrangement. For instance, instead of measuring temperature of supply air right after recuperator, sensor is usually placed only after heater (cooler). Also exhaust air temperature before recuperator is often remains unmeasured. In this case thermometer inside ventilated room could be used instead. Such suboptimal placement of sensors can cause drop in flow rate estimation accuracy as temperatures of flows will be affected with fans waste heat, imperfections of heat insulation of ducts and other factors. Influence of alternative sensors positions will be examine further on data from previously conducted experiments, in first each measuring point will be replaced separately, then combination of alternative sensors

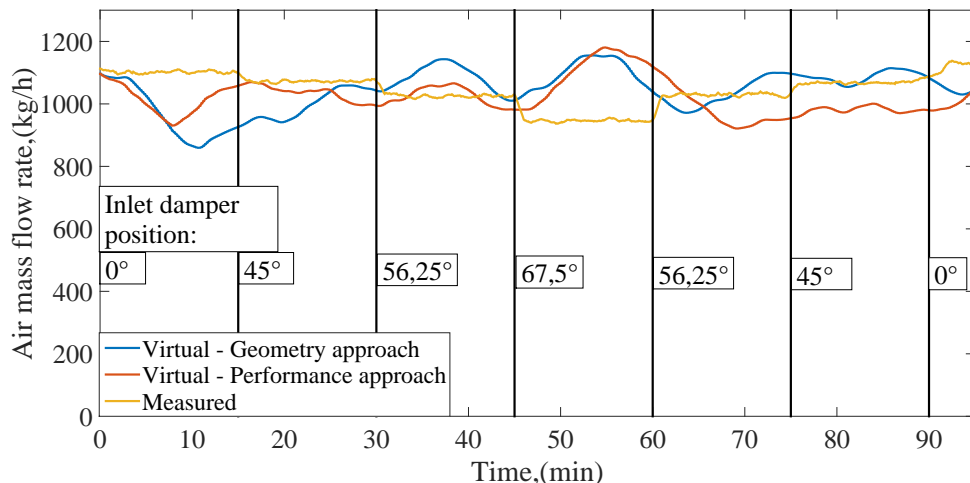


Figure 25 Exhaust mass airflows - experiment 5.05.2015 - filtered

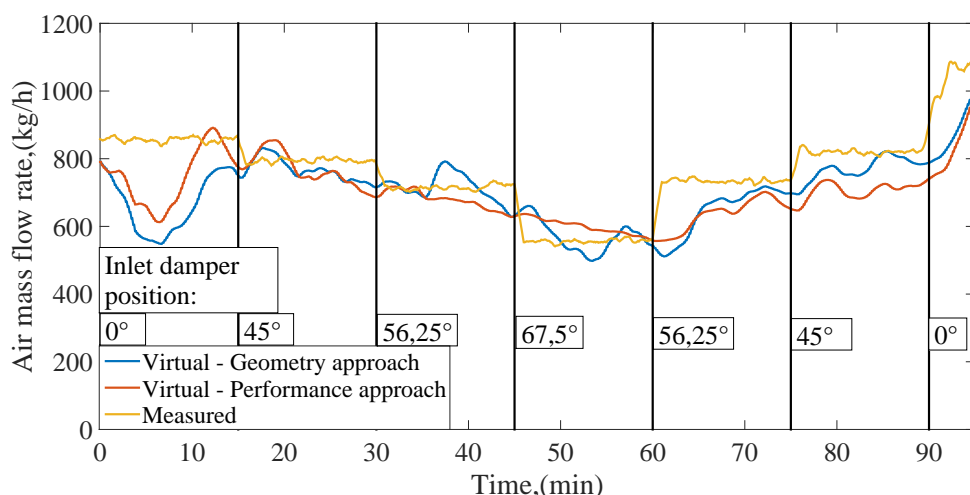


Figure 26 Supply mass airflows - experiment 5.05.2015 - filtered

will be tested. Temperature curves from all available thermometers are presented on following figure (measurement points are numbered according to fig.11).

As can be seen on figure, all pairs of thermometers have similar reading except of pair Thermometer 3 - Thermometer 6 due to turned on heater.

Since geometry and performance curve approaches based on similar physical dependencies, it is assumed that new sensors positions will have same impact on both models. According to that assumption comparison results will be presented only for geometry approach for sake of research clearness. Only last comparison will be carried out for both approaches

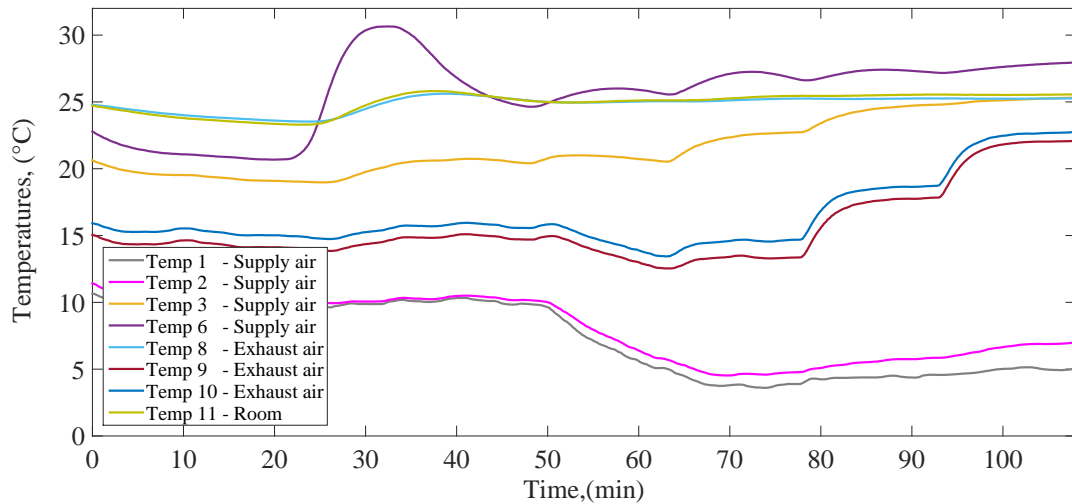


Figure 27 Temperatures during 1.4.2015 experiment

4.5.1 Supply air temperature in front of HRV

This thermometer (numbered as "2" at fig. 11) was replaced with one at the very start of inlet duct (point "1" at fig. 11), which basically measures outdoor temperature.

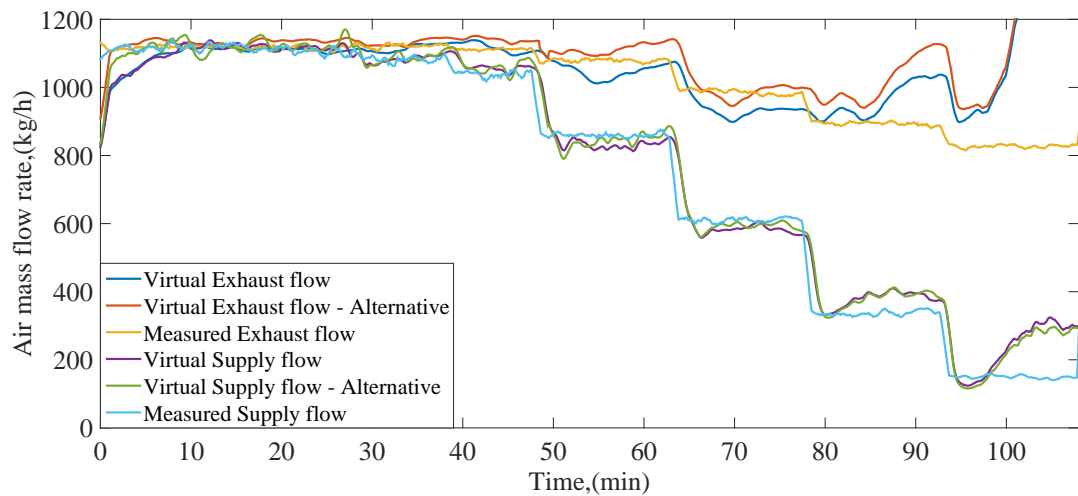


Figure 28 1.4.2015 experiment - Thermometer 1

Since there are no significant heat sources between those two sensors, their readings are pretty close. Replacement caused 2.5% increase in uncertainty for exhaust air and 0.4% for supply air.

4.5.2 Supply air temperature behind HRV

This thermometer (numbered as "3" at fig. 11) was replaced with one at the end of inlet duct (point "6" at fig. 11), which measures temperature before it comes to room.

Since readings of this sensor were affected by turned on heater model was unable to estimate flow rate.

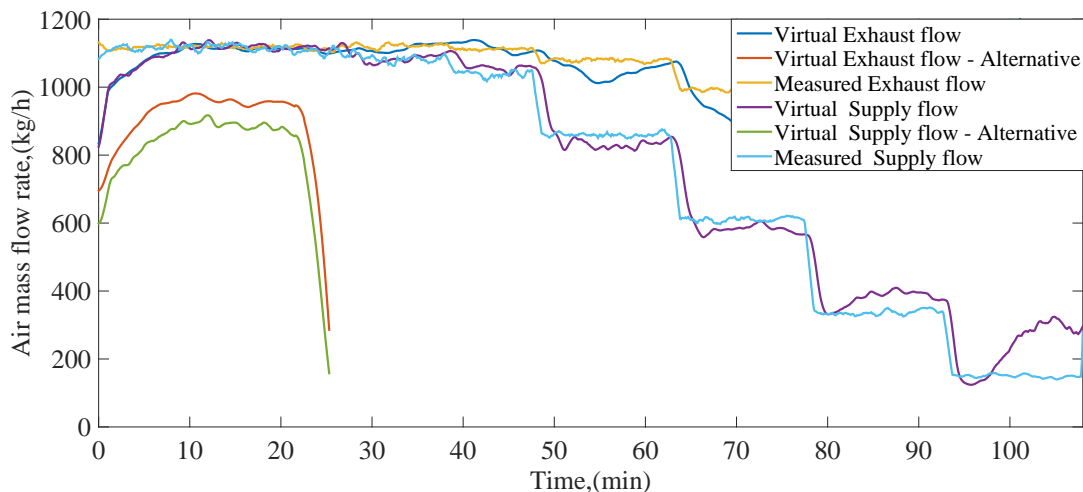


Figure 29 1.4.2015 experiment - Thermometer 6

4.5.3 Exhaust air temperature in front of HRV

This thermometer (numbered as "8" at fig. 11) was replaced with one in the testing chamber (point "11"), which measures temperature of indoor air.

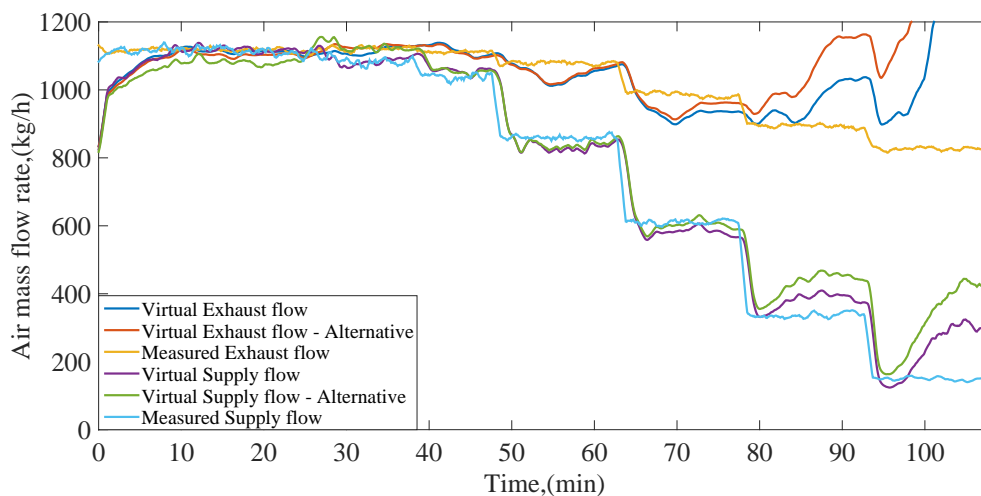


Figure 30 1.4.2015 experiment - Thermometer 11

Affect of this replacement on flow rate estimation is stronger than with Temp 1 sensor, although supply flow changes are still recognizable from graph. Replacement caused 10.7% increase in uncertainty for exhaust air and 3.4% for supply air.

4.5.4 Exhaust air temperature behind HRV

This thermometer (numbered as "9" at fig. 11) was replaced with one at the end of exhaust duct (point "10" at fig. 11).

Affect of this replacement on flow rate estimation is very strong, especially on exhaust air flow rate readings, although supply flow changes are still recognizable from graph.

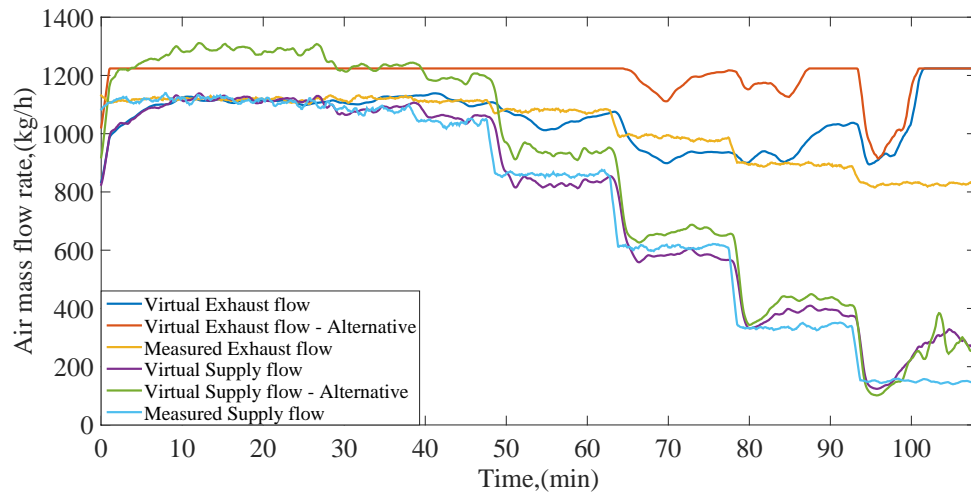


Figure 31 1.4.2015 experiment - Thermometer 10

Replacement caused 25.1% increase in uncertainty for exhaust air and 6.8% for supply air.

4.5.5 Combination of alternative sensors

For this test readings from Thermometers 2, 8 and 9 were respectively replaced with Thermometers 1, 11 and 10 to examine simultaneous influence of such replacements.

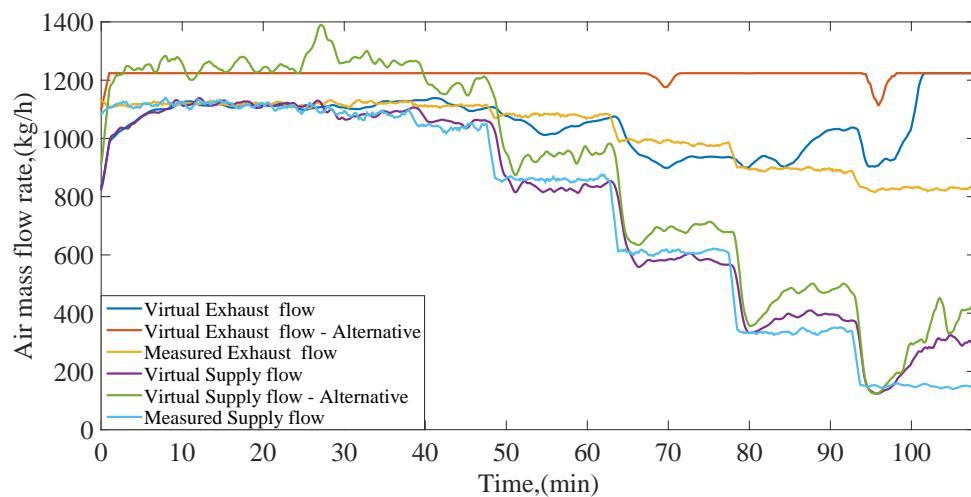


Figure 32 1.4.2015 experiment - Thermometers 1, 11 and 10

Although supply flow changes are still recognizable from graph, relative uncertainty of 14.4% might be unacceptable for majority of applications.

4.5.6 Combination of alternative sensors with corrections

This test was conducted with same sensors arrangement as previous one, but some corrections of thermometers reading were made. Here simple calibrations were made,

applicable only for exact laboratory conditions. Aim of this test was to demonstrate possibility of more precise measurement with alternative sensors positioning. To reach better estimation accuracy for commercial solutions, more sophisticated methods of virtual calibration or outputs from other virtual sensors [12] could be used.

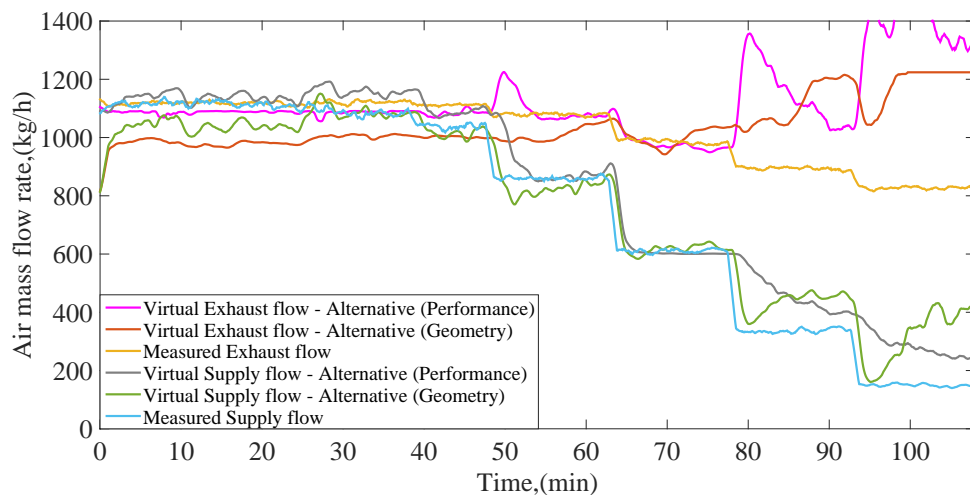


Figure 33 1.4.2015 experiment - Thermometers 1, 11 and 10 with corrections

As can be seen of fig. 33, even with simple calibration of thermometers it is possible to increase virtual sensor accuracy by 4.8% (for supply flow). Also results of modeling with performance curve approach are presented on figure.

4.6 Bypass leakage simulation

At certain times of the year it is more thermally efficient to bypass the recuperator. In the summer it is reasonable when so-called night cooling is used. In autumn and spring there may be no thermal benefit from the recuperation—it may heat/cool the air too much and it will be better to use external air directly. [13] In ACU it is managed with additional bypassing duct and regulating damper. Although it creates an obstacle for flow rate estimation using proposed method, since no air is flowing through HRV.

Aim of this test is to check if opened bypass can be exposed clearly on sensors readings. During the experiment bypass damper was opened and then fully closed.

Open bypass state is clearly recognizable from both sensors readings, though geometry approach model has longer settling time.

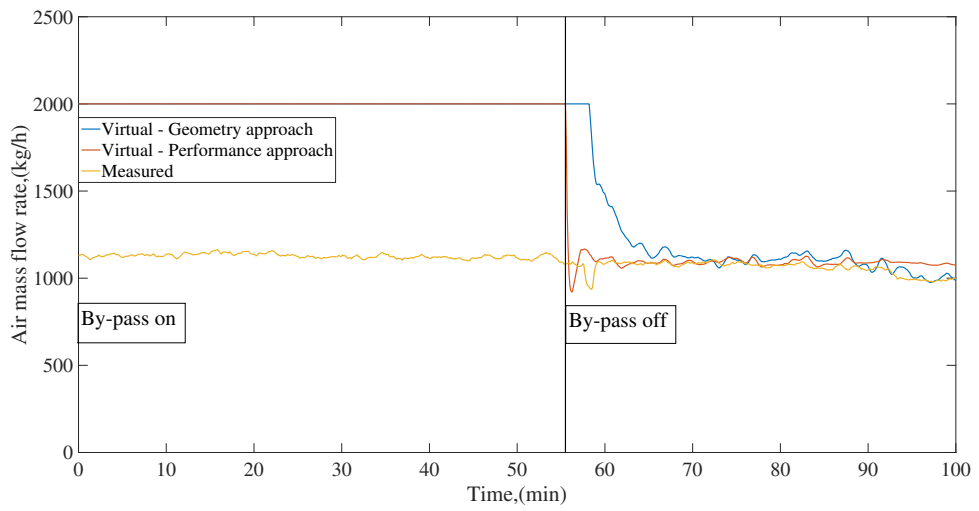


Figure 34 Exhaust mass airflows - open bypass

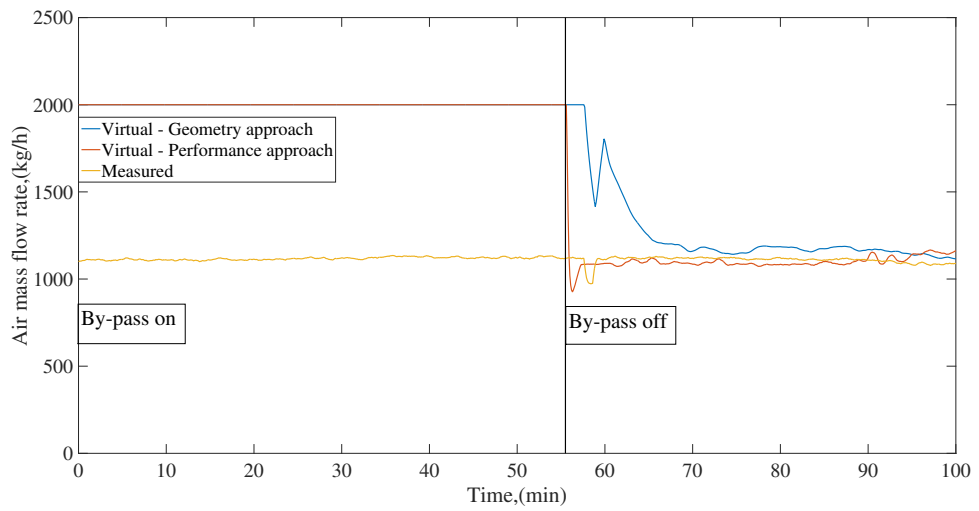


Figure 35 Supply mass airflows - open bypass

5 Scenarios of commercial utilization

The proposed virtual air mass flow rate sensor could be useful in following situations:

- **For advanced automatic control purposes:** regulators ensuring consistency of air temperature (by shifting heater or cooler valve) could be adjusted according to flow rate. Potentially it can increase control efficiency and reduce heat consumption.
- **For remote troubleshooting and technical support:** knowledge of air flow rates simplifies system analysis and fault diagnosis and potentially could reduce maintenance cost by minimizing necessity of travel to object.
- **For on-line fault detection and diagnostics:** method has certain limitations reducing its accuracy, according to that, two types of FDD algorithms could be used:
 - **Active FDD:** Here by *active* was meant ability of the system to temporally adjust control signals with the aim of measurement accuracy increase.
 - **Passive FDD:** Such algorithm can not interfere in automatic control process and can only monitor control signals and other sensors readings to detect virtual sensor accuracy loss.

Both introduced methods of Fault Detection and Diagnosis based on the Virtual Sensor could use either geometry or performance curve approach and will be described in this chapter further.

5.1 Passive FDD algorithm

Following factors could reduce (in extreme cases down to zero) accuracy of virtual sensor:

- Open by-pass: open or semi-open by-pass damper significantly affects VS accuracy, since only air flowing through HRV can be measured.
- Low or minimal temperature difference between indoor and outdoor air temperatures: in such conditions heat exchange process is weakly expressed, which in turn lowers accuracy of VS
- In case when second temperature sensor of supply air is placed behind heater (and chiller), turned on heating (cooling) makes impossible to estimate flow rate.
- Air flow in one direction is noticeably faster than in other.

To avoid false alarms of FDD, listed factors should be detected opportunely. It could be reached by temperatures analysis and also with control signals monitoring. Generic algorithm of such FDD is presented at fig.36

Necessary HRV parameters (performance curve or dimensions depending on chosen approach) could be entered manually or automatically gained from Building Information Model (BIM).

BIMs are files which can be exchanged or networked containing information concerning physical and functional characteristics of places. One of most popular BIM format used worldwide is IFC4.

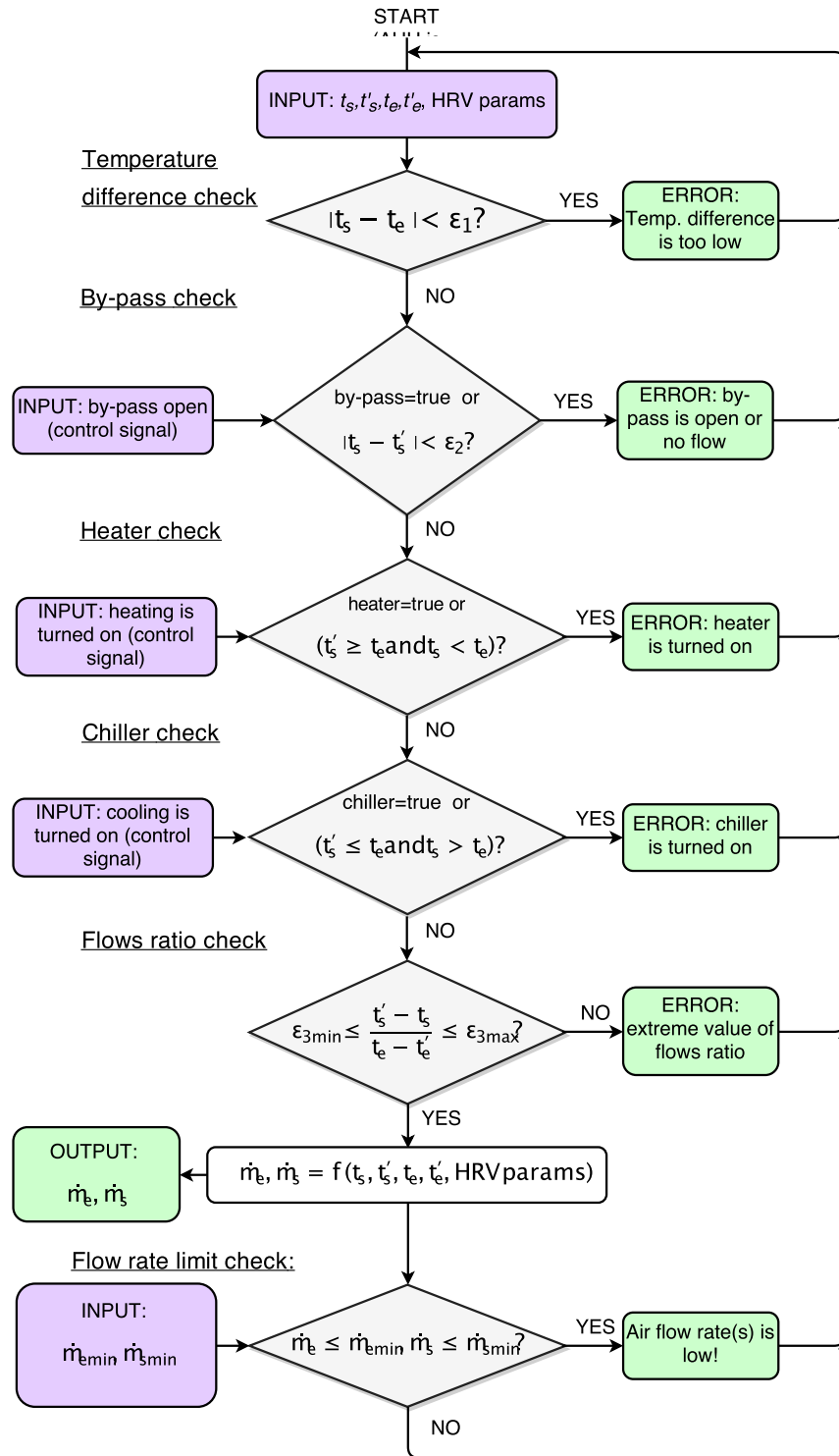


Figure 36 FDD algorithm scheme - passive method

5.2 Active FDD algorithm

In contrast to passive one, active FDD algorithm does not run permanently and could be started on demand or regularly on schedule. When started algorithm provides some

adjustments of the system, according to preset routine: it can turn off heating, close by-pass damper if opened or others. Aim of this measures is to create better conditions for flow rate estimation by excluding factors listed in previous section. After test routine has finished system settings will be restored to original state. Such tests could be conducted periodically (once a week, month), when building is not occupied (at night time) or on demand if AHU failure is suspected. Normally, test routine can take approximately 30min including time needed for temperatures stabilization.

Generic algorithm of active FDD is presented at fig.37

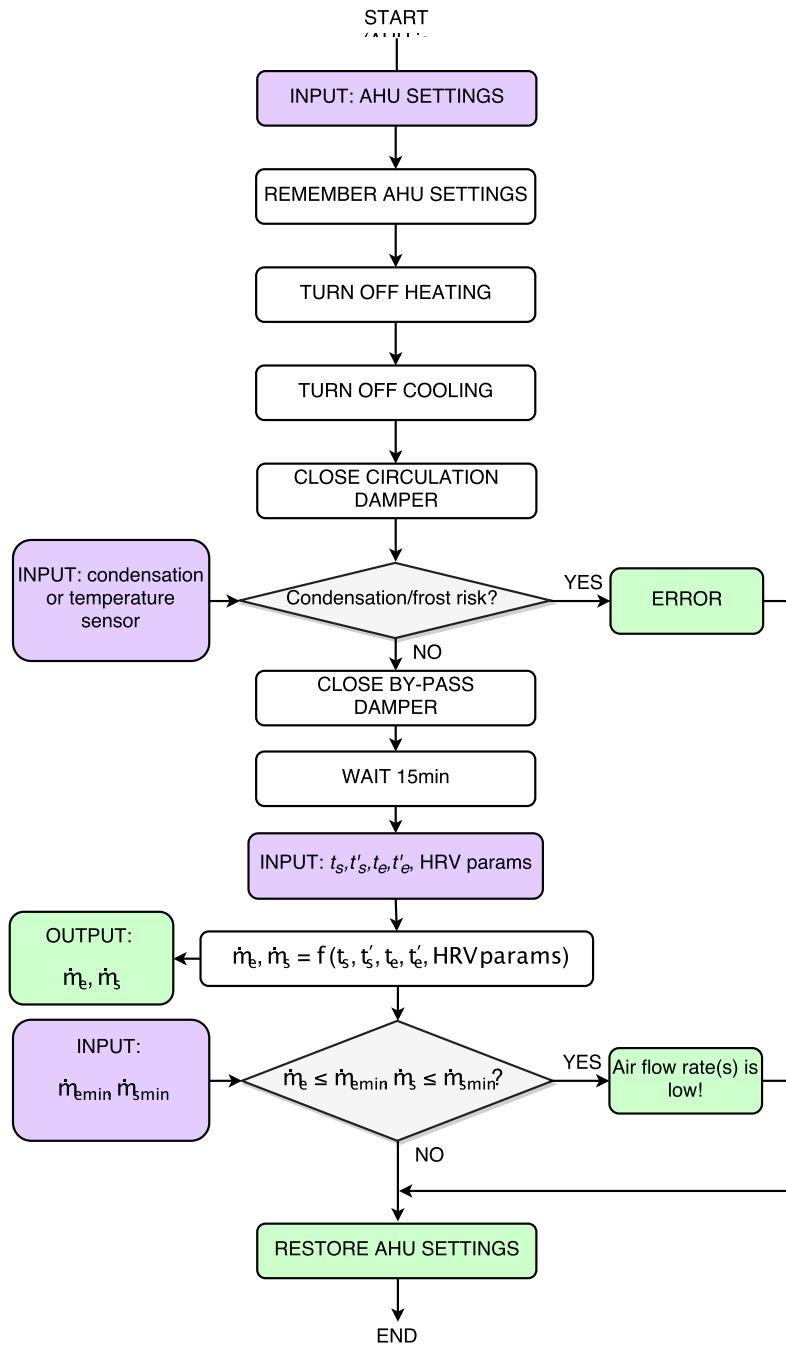


Figure 37 FDD algorithm scheme - active method

Also combination of passive and active FDD algorithms can be used: passive algorithm runs permanently till one of mentioned factors is detected, in this case system warns user about decreased accuracy and asks if active test should be conducted for more precise flow rate estimation.

5.3 Implementation of VS on Programmable Logic Controller Tecomat Foxtrot

As was mentioned Virtual Sensor calculation model can be converted to program code recognizable by Programmable Logic Controllers (PLC) and run directly on such devices. It could be effective since such devices are often used as main computation unit for modern Building Automation Systems, so no additional hardware is required.

In this section example of such program will be presented: PLC Tecomat Foxtrot from Czech manufacturer Teco has been chosen as a platform. Program will be based on performance curve approach and passive FDD algorithm.

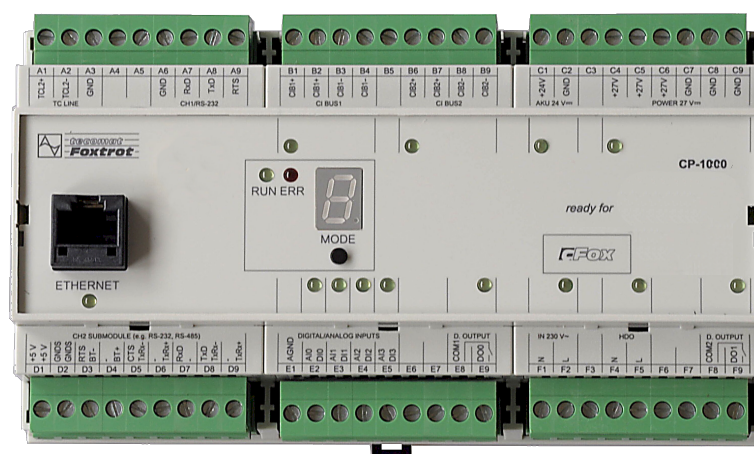


Figure 38 Tecomat Foxtrot Central Unit CP-1000 [18]

Tecomat Foxtrot is a small modular control system consisted of central unit and peripheral I/O modules interconnected with communicational bus. System support both analogue and digital inputs and outputs and can communicate with majority of HVAC devices using such protocols as TCP/IP, Modbus, KNX, OpenTherm and others. Programs for Tecomat systems can be written and debugged using software called Mosaic. Tecomat Foxtrot respects standard IEC61131-3. that means program can be described in four programming languages (including two graphical). Central unit also has SD-card slot to store data and built-in web server on which visual human-machine interface is based. This PLC is widely used to control building technologies in Czech Republic and abroad. [18]

The program consists of three main parts:

- **Virtual sensor model** written in Continuous Function Chart (CFC) language (fig.39)
- **FDD algorithm** written in Structured Text (ST) language (Appendix B)
- **Visualization** - simple HMI representing simplified AHU scheme which allows user to monitor current state of the unit (fig.40).

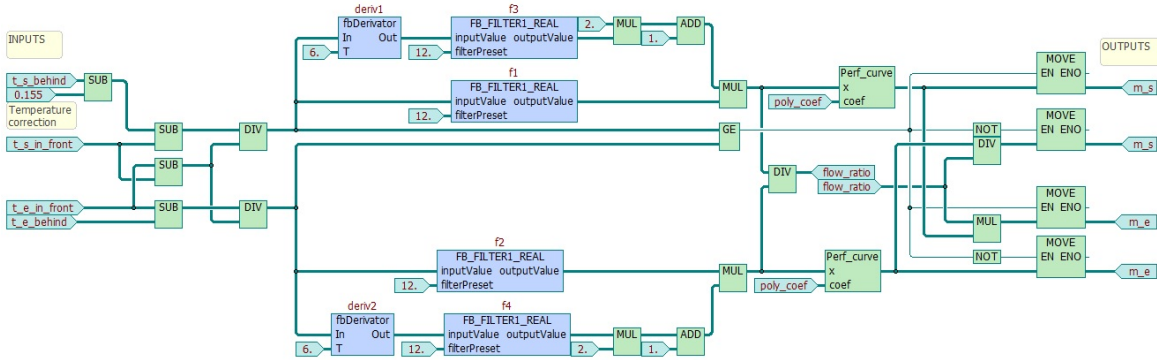


Figure 39 Virtual sensor model in CFC language

All sensors readings are additionally logged on SD-card in a form of .CSV (open text format) file and can be download via visualization for further analysis. Also PLC can send e-mail or SMS notifications containing current system state or in case of failure.

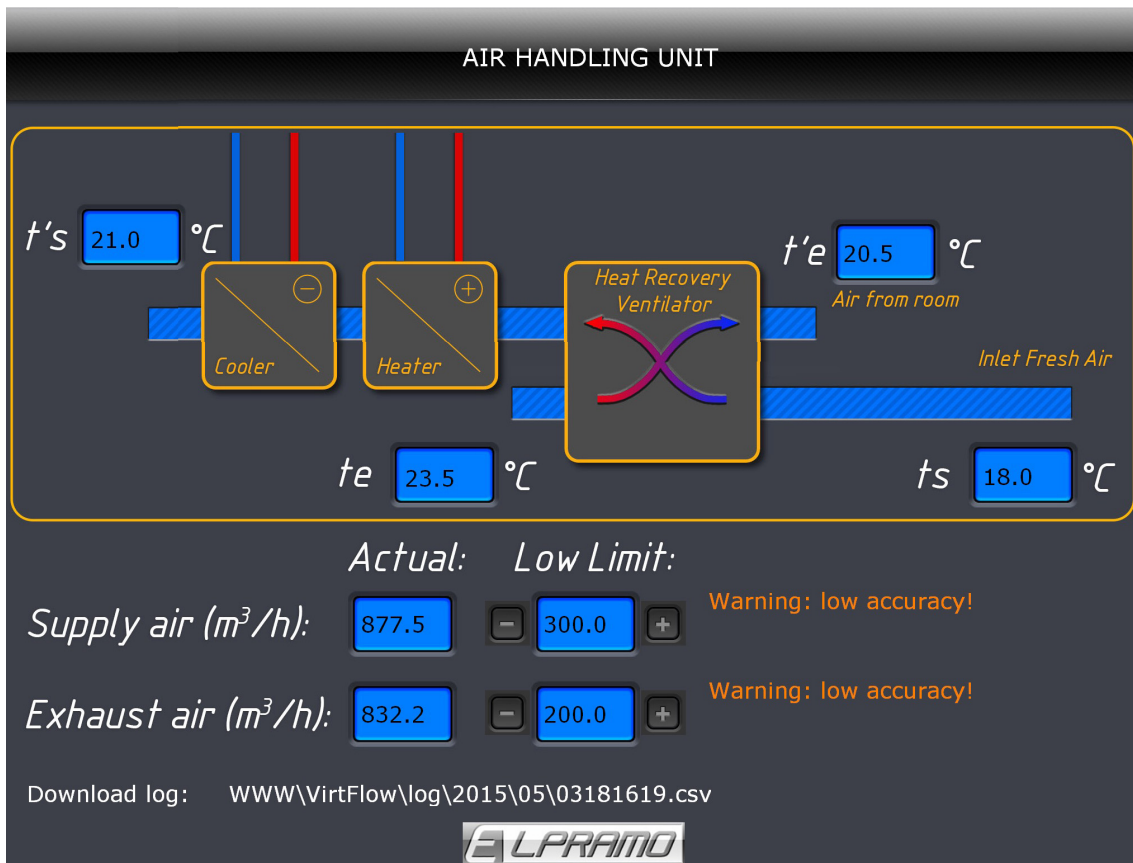


Figure 40 Web interface of FDD system

6 Conclusion

Designed Virtual Sensor of air flow mass rate inside Air-Conditioning Unit successfully overcame majority of laboratory tests: virtually estimated values of flow rate were close to measured ones throughout the whole range of fans speed. During number of tests mass flow rate of supply air was estimated with higher accuracy than flow rate of exhaust air. This can be explained by the fact that exhaust flow rate was noticeably faster than the supply one (since regulating damper was installed only on supply duct). The other version is that one of the sensors has been influenced by some factor. Although, even taking into account this weakness the Virtual Sensor still could be a useful element of future HVAC systems: knowledge of supply flow rate is more desirable since it directly affects behavior of heating/cooling and other subsystems installed on supply duct.

Such typical ACU failures as clogged ducts, stuck dampers or damaged fans could be successfully exposed from VS readings. Timely detection of this failures could prevent unnecessary heat/cool overconsumption and as a result decrease operational cost of ventilation system. Besides proposed VS requires minimum or none of additional hardware, which also contributes to financial benefits of method's implementation.

Uniqueness of the method consists of the fact that Heat Recovery Ventilator (or Recuperator) is used as basis for Virtual flow rate Sensor. Such devices are widely used as part of commercial ACUs and have simple construction, which provides stable results along entire life-cycle, simplifies calculations and allows to use one computational model for wide range of systems without serious changes in program. No long learning data is required for method, as in case of Black-box models, though some system-specific calibration can improve VS performance. Method itself requires only four temperature measurements and knowledge of HRV parameters. Those thermometers are typically installed in ACU by default or can be easily installed if not, in contrast to physical flow rate sensors. Depending on form in which HRV parameters are represented, one of two proposed approaches can be used: both HRV geometry and Performance Curves approaches showed similar accuracy in normal conditions.

Experiments conducted on testing rig helped to estimate VS accuracy, although it was unable to evaluate sensor precisely: installed physical anemometers provide measurements with high uncertainty due to methodological limitations, so strictly speaking their reading are not fully trustworthy.

In previous chapter it was shown that VS can be integrated into Fault Detection and Diagnostic System and without significant difficulties can be implemented on PLC-controlled Automation System. That fact also increases commercial potential of method.

Additional method assessment will be given in following two sections.

6.1 Discovered weaknesses and features of approach

Though VS demonstrated good overall performance along laboratory tests in appropriate conditions, undoubtedly, it has certain disadvantages:

- Accuracy depends on temperature difference between outdoor and indoor air: the lower difference is - the higher uncertainty is. Basically it means that in moderate

climate conditions VS could have lower accuracy during spring and autumn, also accuracy fluctuations along the daytime are possible. Unfortunately, this limitation is fundamental and can only be suppressed but not fully removed.

- Since some simplifications have been made, method can not guarantee accurate outputs for any type of HRV without preliminary calibration and validation using physical flow rate sensor
- Standard AHU technical documentation do not provide sufficient amount of information for VS. That could be a problem especially for older air handling units taken out of production.
- Still there are factors negatively influencing accuracy of sensor that hardly can be revealed: partly opened by-pass or circulation damper, residual heat in heater or small ACU leakage could affect readings and remain undiscovered.
- Although sensor provide sufficient accuracy for FDD, it questionable that it would be enough to use it for automatic control, that is more demanding especially in terms of dynamic qualities of sensors.
- If heat exchanger in ACU will be replaced with newer one, which has even slightly different parameters, model should be readjusted according to changes and validated again.
- Precise temperature measurements are strongly advised: 0.5K error in temperature measurement causes noticeable deviation in VS readings. Modern thermometers (such are Pt1000) provide sufficient accuracy so the critical factor here is correct sensor placement and elimination of external influences.

Resuming listed disadvantages should be mentioned, that physical air flow measurements also have their weaknesses and even in state as it is now, described Virtual Sensor can be competitive to other methods of flow rate estimation.

6.2 Proposed improvements

One of unmentioned method's benefits is flexibility: used models equations can be gradually improved and refined without major approach changes. So listed weaknesses could be minimized in future.

- Reconsider used physical simplifications:
 - Include influence of air humidity and pressure. Those quantities could be in turn measured with virtual sensors, atmospheric pressure could also be gained from weather web-servers, that provides on-line data.
 - Study model behavior for condensation or frost state so antifreeze protection failure could be detected.
 - Even so-called counter-current heat exchangers have cross-current parts at their ends, so respective corrections could be made.
 - Used empirical equations (Reynolds and Nusselt numbers calculations) could be corrected to better match exact HRV geometry.
- Performance Curve for testing rig could be measured more accurately with more precise control of fans speed.
- When alternative sensors positions are used, advanced virtual calibration methods could be built-in Virtual Sensor to reach better results.
- Model could be expanded by equations for other HRV geometries, such are cross-current arrangement, different shapes of fins etc.
- Conduct experiments on several different AHUs and also make test on functioning systems of real buildings outside laboratories.

- Usage of more precise physical flow rate sensors should be considered for better evaluation of VS
- Alternative methods of air flow rate estimation could be studied and applied as secondary Virtual Sensors: that can be useful in periods, when described VS is not accurate.
- Virtual Sensor could be tested not only as stand-alone device but also as part of Fault Detection or Control System.
- Create self-contained application based on Simulink model, so no additional software is required for sensor to operate.
- Possibility of VS implementation not only on PLCs but also on built-in AHU's control unit should be tested. This research requires collaboration with manufacturers of recuperators.

Some of listed ways to improve Virtual Sensor require serious amount of work and advanced measurement techniques, so economical effort should always be weighted.

Bibliography

- [1] S. Katipamula and M. R. Brambley. “Methods for Fault Detection, Diagnostics, and Prognostics for Building Systems— A Review, Part I”. In: *HVAC and R Research* 11.1 (2005), pp. 3–25.
- [2] H. Li, D. Yu, and J. E. Braun. “A review of virtual sensing technology and application in building systems”. In: *HVAC and R Research* 17.5 (2011), pp. 619–645.
- [3] V. Venkatasubramanian et al. “A review of process fault detection and diagnosis. Part I: Quantitative model-based methods”. In: *Computers and Chemical Engineering* 27.3 (2003).
- [4] D. Yu, H. Li, and M. Yang. “A virtual supply airflow rate meter for rooftop air-conditioning units”. In: *Building and Environment* 46 (2011), pp. 1292–1302.
- [5] N.V. Suryanarayana. “Heat and Mass Transfer” - Mechanical Engineering Handbook”. In: ed. by Frank Kreith. Boca Raton: CRC Press LLC, 1999, pp. 46–55.
- [6] H. Li and J.E. Braun. “Economic evaluation of benefits associated with automated fault detection and diagnosis in rooftop air conditioners”. In: *ASHRAE Transactions* 113.2 (2007), pp. 200–210.
- [7] W. Zhang et al. “Virtual sensors design in vehicle sideslip angle and velocity of the centre of gravity estimation.” In: *9th International Conference on Electronic Measurement & Instruments* (Aug. 2009).
- [8] M.D. Gustafsson et al. *Virtual sensors of tire pressure and road friction*. Tech. rep. Society of Automotive Engineers, Inc., 2001.
- [9] M. Ward and J. Siegel. “Modeling filter bypass: Impact on filter efficiency.” In: *ASHRAE Transactions* 111.1 (2005), pp. 1091–1100.
- [10] H. Li and J.E. Braun. “A methodology for diagnosing multiple-simultaneous faults in vapor compression air conditioners”. In: *HVAC and R Research* 13.2 (2007), pp. 369–395.
- [11] H. Li and J.E. Braun. “Decoupling features for diagnosis of reversing and check valve faults in heat pumps”. In: *International Journal of Refrigeration* 32 (2009), pp. 316–326.
- [12] H. Yang and H. Li. “A generic rating-data-based DX coil modeling method”. In: *HVAC and R Research* 16.3 (2010), pp. 331–353.
- [13] F. DRKAL et al. “Vzduchotechnika”. In: Evropský sociální fond, 2010. Chap. Zpětné získávání tepla, pp. 54–60.
- [14] tzb-info.cz. *Trh vzduchotechniky a klimatizace v Německu a energetická účinnost centrálních větracích a klimatizačních zařízení*. URL: <http://vetrani.tzb-info.cz/vzduchotechnicka-zarizeni/5516-trh-vzduchotechniky-a-klimatizace-v-nemecku-a-energeticka-ucinnost-centralnich-vetracich-a-klimatizacnich-zarizeni> (visited on 2015).

- [15] K. Hemzal. “Přenosové jevy v technice prostředí”. In: ČVUT, 2004. Chap. Vyměňíky tepla.
- [16] V. Horyna and O. Hanus. “Air handling unit test rig for research and development of fault detection and diagnostics methods”. In: *POSTER* (May 2014).
- [17] Tomáš Matuška and Luděk Mareš. “Experimentální metody 1”. In: Evropský sociální fond, 2009. Chap. Termoanemometry, pp. 43–44.
- [18] Teco a.s. *Tecomat Foxtrot - popis*. URL: <http://www.tecomat.com/index.php?ID=388> (visited on 2015).

Appendix A

Simulink Diagram - Geometry approach

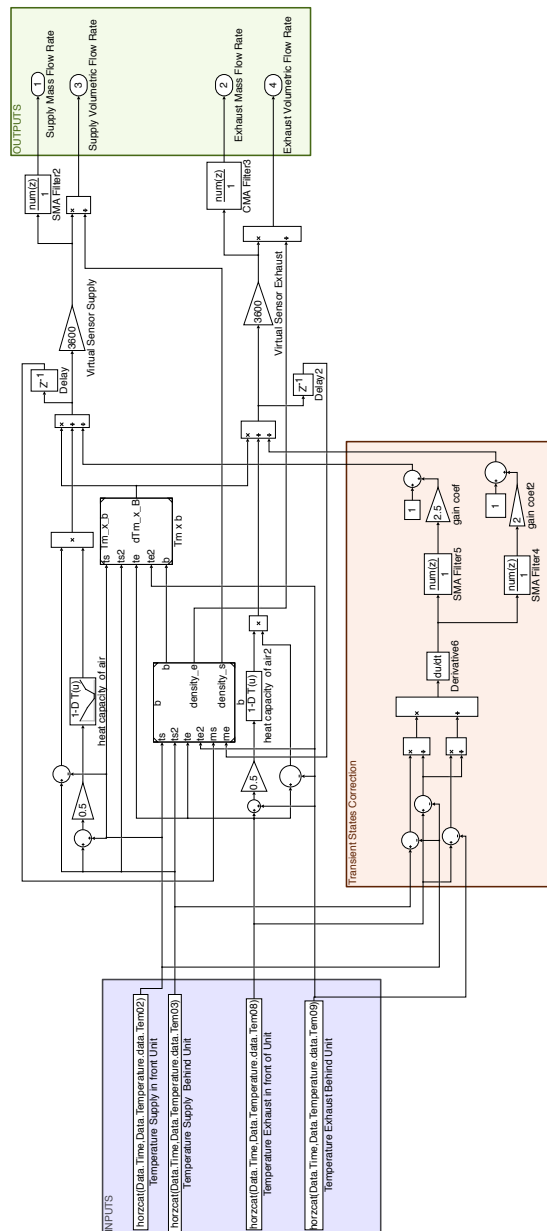


Figure 41 Overall Simulink diagram - geometry approach.

Appendix B

Program for PLC source code

Below program code written in Structured Text language is presented. This code can be compiled with Mosaic software into program for PLC Tecomat Foxtrot and used as simple Fault Detection and Diagnosis algorithm.

```
PROGRAM prgMain
low_difference :=false;
bypass:=false;
heater:=false;
cooler:=false;
other_err:=false;
m_s_low:=false;
m_e_low:=false;
m_s_ok:=true;
m_e_ok:=true;
m_s_low_acc:=false;
m_e_low_acc:=false;

if abs(t_e_in_front-t_s_in_front)<4.
then low_difference:=true;
end_if; //sensor is not accurate when temp.difference is extremely low

if abs(t_e_in_front-t_s_in_front)<6. and not low_difference
then m_s_low_acc:=true; m_e_low_acc:=true;
end_if; //sensor accurasy is decreased when temp.difference is low

if abs(t_s_behind-t_s_in_front) <1. then //open by-bass detection
    if abs(t_e_in_front-t_s_behind)>abs(t_s_behind-t_s_in_front)
    then bypass:=true;
    else other_err:=true;
    end_if;
end_if;

if not bypass then //sensor is not accurate if heating or cooling is on
    if t_s_behind>=t_e_in_front and t_s_in_front<t_e_in_front
    then heater:=true;
    end_if;
    if t_s_behind<=t_e_in_front and t_s_in_front>t_e_in_front
    then cooler:=true;
    end_if;
end_if;
```

Appendix B Program for PLC source code

```
if (flow_ratio<0.3 or flow_ratio>1.7) and m_s_ok
then m_s_low_acc:=true;
end_if; //accuracy is decreased if one flow is noticeably faster than the other

if (flow_ratio<0.5 or flow_ratio>2.) and m_e_ok
then m_e_low_acc:=true;
end_if;

if (flow_ratio<0.1 or flow_ratio>4.)
then m_s_ok:=false;
end_if;

if (flow_ratio<0.3 or flow_ratio>8.)
then m_e_ok:=false;
end_if;

if other_err or bypass or heater or cooler or low_difference
then m_s_ok:=false; m_s_low_acc:=false;
      m_e_ok:=false; m_e_low_acc:=false;
end_if;

if m_s<m_s_limit and m_s_ok and not m_s_low_acc
then m_s_low:=true;
end_if; //duct is clogged if airflow is low and sensor is accurate

if m_e<m_e_limit and m_e_ok and not m_e_low_acc
then m_e_low:=true;
end_if;
END_PROGRAM
```